Neurobiology of Disease 148 (2021) 105214

Contents lists available at ScienceDirect

Neurobiology of Disease

journal homepage: www.elsevier.com/locate/ynbdi

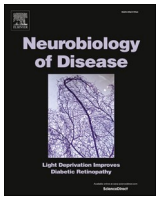

Dopaminergic denervation impairs cortical motor and associative/limbic information processing through the basal ganglia and its modulation by the CB1 receptor

Mario Antonazzo [a,b], Sonia María Gomez-Urquijo [c,d], Luisa Ugedo [a,b], Teresa Morera-Herreras [a,b,*]

[a] Department of Pharmacology, Faculty of Medicine and Nursing, University of the Basque Country (UPV/EHU), Leioa 48940, Spain
[b] Neurodegenerative diseases Group, Biocruces Health Research Institute, Barakaldo, Bizkaia, Spain
[c] Department of Neurosciences, Faculty of Medicine and Nursing, University of the Basque Country (UPV/EHU), Leioa 48940, Spain
[d] Achucarro Basque Center for Neuroscience, Science Park of the University of the Basque Country (UPV/EHU), Leioa 48940, Spain

ARTICLE INFO

Keywords:
Cannabinoid
Basal ganglia
Substantia nigra pars reticulata
Sensorimotor circuit
Prefrontal circuit
Electrophysiology

ABSTRACT

The basal ganglia (BG) are involved in cognitive/motivational functions in addition to movement control. Thus, BG segregated circuits, the sensorimotor (SM) and medial prefrontal (mPF) circuits, process different functional domains, such as motor and cognitive/motivational behaviours, respectively. With a high presence in the BG, the CB1 cannabinoid receptor modulates BG circuits. Furthermore, dopamine (DA), one of the principal neurotransmitters in the BG, also plays a key role in circuit functionality. Taking into account the interaction between DA and the endocannabinoid system at the BG level, we investigated the functioning of BG circuits and their modulation by the CB1 receptor under DA-depleted conditions. We performed single-unit extracellular recordings of *substantia nigra pars reticulata* (SNr) neurons with simultaneous cortical stimulation in sham and 6-hydroxydopamine (6-OHDA)-lesioned rats, together with immunohistochemical assays. We showed that DA loss alters cortico-nigral information processing in both circuits, with a predominant transmission through the hyperdirect pathway in the SM circuit and an increased transmission through the direct pathway in the mPF circuit. Moreover, although DA denervation does not change CB1 receptor density, it impairs its functionality, leading to a lack of modulation. These data highlight an abnormal transfer of information through the associative/limbic domains after DA denervation that may be related to the non-motor symptoms manifested by Parkinson's disease patients.

1. Introduction

Although, for a long time, the basal ganglia (BG) have been viewed exclusively as motor control structures, they are a highly organized network that integrates information from several cortical areas, conforming to segregated parallel anatomical circuits that process different functional domains. Thus, while sensorimotor (SM) circuits play a crucial role in motor functions, medial prefrontal (mPF) circuits are related to cognitive and motivational information processing (Alexander et al., 1986; Haber, 2003; Middleton and Strick, 2000; Parent and Hazrati, 1995). CB1 cannabinoid receptors are highly expressed in the BG, as well as in other parts of the brain (Herkenham et al., 1991; Köfalvi et al., 2005; Mailleux and Vanderhaeghen, 1992; Julián Romero et al., 2002; Tsou et al., 1998). Interestingly, CB1 receptor activation differentially modulates cortical information transfer through both circuits, decreasing SM information transmission through the trans-striatal pathways and profoundly hindering cortico-nigral transmission through the mPF circuits (Antonazzo et al., 2019). Some of the effects found after acute and chronic exposure to cannabis extracts, such as motor performance deficits (slower reaction time or inappropriate motor coordination) and neurocognitive functioning impairments (in memory, associative learning, task switching or attention) (Grant et al., 2003; Prashad and Filbey, 2017; Schreiner and Dunn, 2012), have been related to the activation of the CB1 receptor.

* Corresponding author at: Department of Pharmacology, Faculty of Medicine and Nursing, University of the Basque Country (UPV/EHU), Barrio Sarriena s/n, Leioa 48940, Spain.
E-mail address: teresa.morera@ehu.eus (T. Morera-Herreras).

https://doi.org/10.1016/j.nbd.2020.105214
Received 12 September 2020; Received in revised form 20 November 2020; Accepted 30 November 2020
Available online 3 December 2020

Dopamine (DA), as one of the principal neurotransmitters in the BG, plays a key role in circuitry functionality (Tremblay et al., 2015). In fact, perturbations in DA neurotransmission at the level of the striatum contribute to maladaptive processing within the BG and lead not only to movement disorders, such as Parkinson's disease (PD), but also to several neuropsychiatric diseases (Tremblay et al., 2015). Substantial evidence supports neuroanatomical and direct/indirect functional interactions between the DA system and the endocannabinoid system in the BG: CB1 receptors form heteromers with DA receptors in striatal projection neurons (Ferré et al., 2009) cannabinoids increase nigrostriatal DA neuronal firing and synaptic DA release in the striatum, mainly through (Morera-Herreras et al., 2012) CB1 receptors present in GABAergic and glutamatergic terminals [for review see (García et al., 2016)] DA modulates endocannabinoid release in the striatum (Giuffrida et al., 1999; Patel et al., 2003); and there is altered endocannabinoid signalling in the BG after DA depletion [details in (Morera-Herreras et al., 2012)].

Considering these findings, we further investigated the impact of DA loss on cortical information transmission through the SM and mPF circuits of the BG and its regulation by the CB1 receptor. For this purpose, simultaneous cortical electrical stimulation and single-unit extracellular recordings of *substantia nigra pars reticulata* (SNr) neurons were carried out in anaesthetized sham and 6-hydroxydopamine (6-OHDA)-lesioned rats.

2. Materials and methods

2.1. Animals

Male Sprague-Dawley rats (160–215 g at the beginning of the experiments) were housed in groups of 4 under standard laboratory conditions (22 ± 1 °C, 55% ± 5% relative humidity, and 12:12 h light/dark cycle) with food and water provided ad libitum. The experimental protocols were reviewed and approved by the Local Ethical Committee for Animal Research of the University of the Basque Country (UPV/EHU, CEEA, ref. ES48/054000/6069). All of the experiments were performed in accordance with the European Community Council Directive on "The Protection of Animals Used for Scientific Purposes" (2010/63/EU) and with Spanish Law (RD 53/2013) for the care and use of laboratory animals.

2.2. Drugs

6-OHDA, desipramine hydrochloride, WIN 55,212-2 and chloral hydrate were obtained from Sigma-Aldrich. AM251 was obtained from Tocris Bioscience. Desipramine and chloral hydrate were prepared in 0.9% saline. 6-OHDA was dissolved in Milli-Q water containing 0.02% ascorbic acid. WIN 55,212-2 and AM251 were diluted in 1:1:18 cremophor/ethanol/saline solution. All drugs were prepared on the day of the experiment.

2.3. 6-Hydroxydopamine lesion

Unilateral 6-OHDA injection in the medial forebrain bundle (MFB) was performed, as previously described (Aristieta et al., 2016, 2019). Thirty minutes before stereotaxic surgery, rats were pretreated with desipramine (25 mg/kg, i.p.) in order to protect noradrenergic terminals from 6-OHDA toxicity. Rats were deeply anaesthetized with isoflurane inhalation (4% for induction; 1.5%–2% for maintenance) and placed in a stereotaxic frame (David Kopf® Instruments). Lesions were performed by two injections of 6-OHDA of 8.75 and 7 μg, respectively (3.5 μg/μl saline with 0.02% ascorbic acid) in the right medial forebrain bundle: 2.5 μl at anteroposterior (AP) −4.4 mm, mediolateral (ML) +1.2 mm and dorsoventral (DV) −7.8 mm, relative to bregma and dura with the toothbar set at −2.4, and 2 μl at AP −4.0 mm, ML +0.8 mm, and DV −8 mm, with toothbar at +3.4 (Paxinos and Watson, 2006). For the administration of the neurotoxin a 10 μl-Hamilton syringe coupled to a pump at an infusion rate of 1 μl/min. Sham animals were similarly treated but instead of 6-OHDA received vehicle. Rats were randomized to receive either vehicle or 6-OHDA infusion. Electrophysiological experiments were performed 4–5 weeks after the lesion.

2.4. Cylinder test

Forelimb use asymmetry was assessed 4 weeks post-surgery as indicative of severe dopaminergic damage using the cylinder test, as previously described (Hernando et al., 2019). Rats were individually placed in a 20 cm diameter methacrylate cylinder and allowed to explore freely. Mirrors were placed behind the cylinder to allow a 360° view of the exploratory behavior. Each animal was left in place until at least 20 supporting front paw touches with open digits were done on the walls of the cylinder. The session was video-recorded for posterior analysis. Touches performed with the front limb contralateral or ipsilateral to the lesioned hemisphere were counted, and data expressed as the percentage of ipsilateral placement. Rats using the ipsilateral paw above 70% were considered to have severe damage of the dopaminergic system. Breakdown of these data into the different experimental groups is found in Table S1 and illustrated in the Fig. 1B.

2.5. Electrophysiological procedures

The electrophysiological procedures, schematically illustrated in Fig. 1, were performed as previously described (Antonazzo et al., 2019). Animals were anaesthetized with chloral hydrate (420 mg/kg, i.p.) for induction, followed by continuous administration (i.p.) of chloral hydrate at a rate of 115.5 mg/kg/h using a peristaltic pump to keep a steady level of anaesthesia. For additional drug administration, the right jugular vein was cannulated. The animal body temperature was maintained at ~37 °C for the entire experiment with a heating pad connected to a rectal probe. The rat was placed in a stereotaxic frame with its head secured in a horizontal orientation. The skull was exposed, and two 3-mm burr holes were drilled over the right SNr and the ipsilateral motor cortex (MC) or anterior cingulate cortex (ACC).

Single-unit extracellular recordings were made by an Omegadot single glass micropipette, pulled with an electrode puller (Narishige Scientific Instrument Lab., PE-2, Japan), broken back to a tip diameter of 1–2.5 μm under a light microscope and filled with 2% Pontamine Sky Blue in 0.5% sodium acetate. This electrode was lowered into the SM (5.8 mm posterior to Bregma, 2.5 mm lateral to midline, and 7–8 mm ventral to the dura mater) or mPF territory (5.4 mm posterior to Bregma, 1.8 mm lateral to midline, and 7–8 mm ventral to the dura mater) of the SNr. To evoke triphasic responses in SNr neurons, the MC (3.5 mm anterior to Bregma, 3.2 mm lateral to midline, and 1.6 mm ventral to the dura mater) or the ACC (2.9 mm anterior to Bregma, 0.6 mm lateral to midline, and 1.7 ventral to the dura mater) ipsilateral to the recording site, was stimulated at 1 Hz (pulse width, 600 μs; intensity, 1 mA) using coaxial stainless-steel electrodes (diameter, 250 μm; tip diameter, 100 μm; tip-to-barrel distance, 300 μm) during the recordings (Cibertec S. A.).

The signal from the recording electrode passed through an AxoClamp 2-B amplifier (Axon Instruments) bridge circuitry, amplified x100, and filtered at 300–3000 Hz with a high-input impedance amplifier (AMPLI64AC, Cibertec). The signal was monitored through an oscilloscope and an audio-monitor. Neuronal spikes were sampled at 25 kHz using a CED micro3 1401 analog-digital interface and a computer running Spike2 acquisition software (Cambridge Electronic Design, UK). SNr neurons were identified as non-dopaminergic by their classically defined electrophysiological characteristics: thin spikes (width, <2 ms) and ability to present relatively high-frequency discharges without decrease in spike amplitude (as described in Antonazzo et al. (2019)). Although multiple neurons were recorded in each animal in order to characterize the spontaneous and cortically evoked activity in both SM

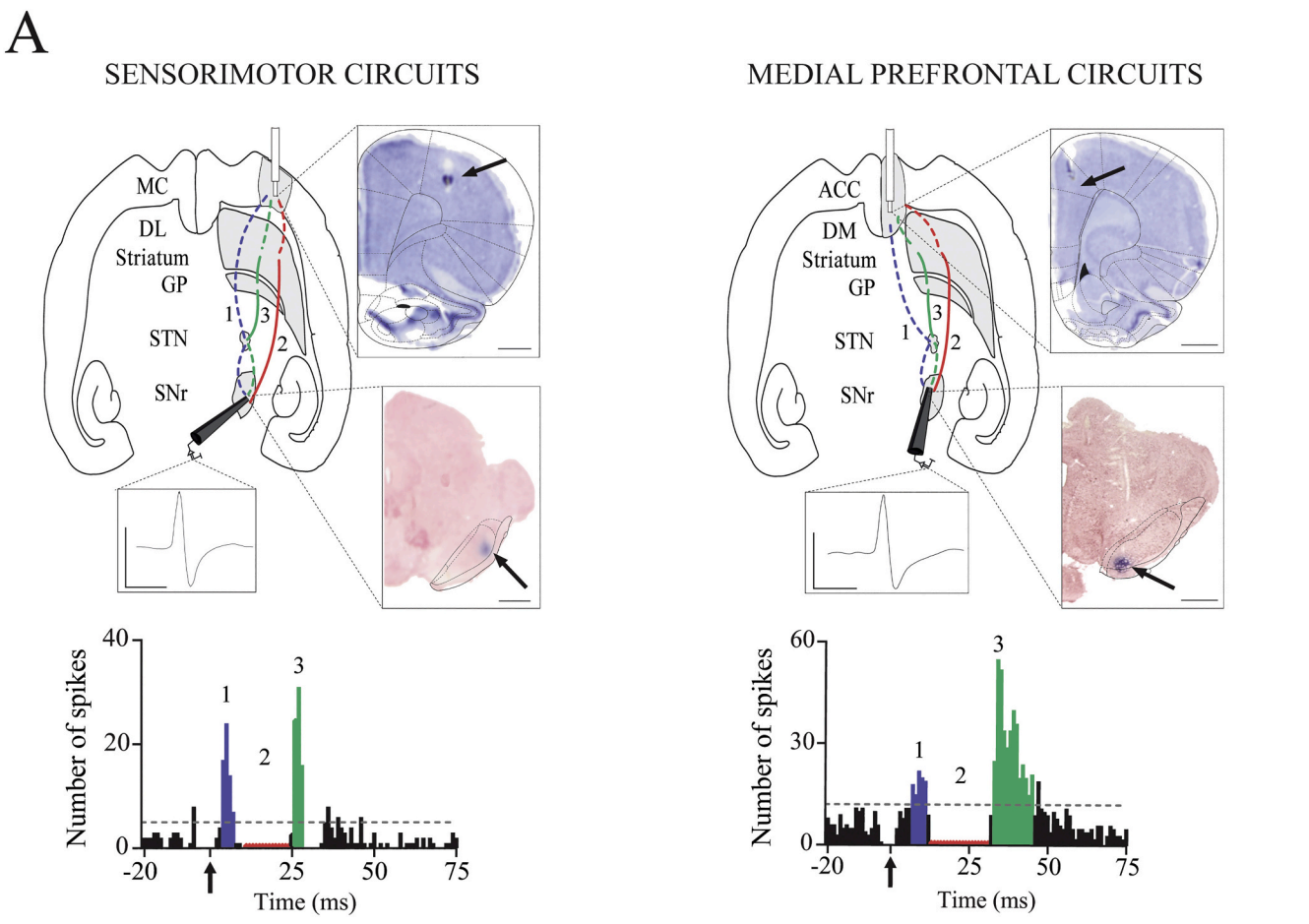

(caption on next page)

Fig. 1. Schematic illustration of electrophysiological recordings in SNr neurons from sensorimotor (SM) and medial prefrontal (mPF) territories, motor asymmetry and dopaminergic denervation in sham and 6-OHDA-lesioned rats.
A. Schematic horizontal sections of the rat brain showing the stimulation of the motor cortex (MC) or the anterior cingulate cortex (ACC), and a representative spike trace from SM-SNr or mPF-SNr neurons during single-unit recordings extracellular. The cortical information is transferred through the (Alexander et al., 1986) hyperdirect (cortex-STN-SNr, in blue), (Anderson et al., 2020) direct (cortex-striatum-SNr, in red) and (Antonazzo et al., 2019) indirect pathways (cortex-striatum-GP-STN-SNr, in green), inducing the characteristic triphasic response in SNr neurons, as illustrated in the peristimulus time histograms. Arrows indicate cortical stimulus application. Scale bar for spike traces is of 1 V and 1 ms. B. Left, video frame showing a rat performing the cylinder test. The mean percentage of ipsilateral forelimb use represented in the bar graph below shows that 6-OHDA-lesioned rats use more the forelimb ipsilateral to the lesioned side, indicating an important degree of motor asymmetry, and suggesting severe dopaminergic denervation. Right, representative brain slices showing TH immunostaining for both sham and 6-OHDA-lesioned rats. Note the severe striatal dopaminergic denervation in 6-OHDA rats, after infusion of the toxin in the MFB. The bar graph below shows the TH optical density (OD) mean percentage of variation, referring to the change in the hemisphere ipsilateral to the lesion vs. the contralateral side. As depicted in the brain slices above, 6-OHDA animals show a severe dopaminergic denervation. Slice scale bars are set to 1 mm. $^{*}P < 0.05$, two-tailed unpaired Student's *t*-test. DL/DM striatum: dorsolateral/dorsomedial striatum; GP: *globus pallidus*; SNr: *substantia nigra pars reticulate*. (For interpretation of the references to colour in this figure legend, the reader is referred to the web version of this article.)

and mPF territories, only one SNr cell was pharmacologically studied per animal.

Firing parameters such as firing rate and coefficient of variation (CV) of SNr neurons were analysed offline using Spike2 software (version 7). The CV consisted on the ratio, expressed as a percentage, between the standard deviation and the mean of the neuron's inter-spike interval histogram. This histogram was made with 1 ms bins, and considering all the inter-spike intervals below 0.5 ms, given the relatively high firing rate of SNr neurons. The existence of burst firing in neurons was determined through a Spike2 script ("surprise.s2s"), based on the Poisson surprise algorithm. These parameters were analysed during time epochs of 150 s under basal conditions, or for 120 s once the drug was administered. Before data analysis, spike-sorting procedures were used just to discriminate electrical stimulation artifacts from actual spikes, and discard them to avoid any interference with posterior analysis. This procedures were done using the Spike2 software, and consisted in principal component analysis and template matching to help discriminate, and group stimulation artifacts and spikes waveforms separately. The few spare waveforms that left ungrouped after this were manually inspected and grouped accordingly. Given the nature of our recordings, only single-units were recorded, and thus all the spikes present in the recordings were from the same unit.

Peristimulus time histograms were generated from 180 stimulation trials using 1 ms bins. The criterion used to determine the existence of an excitatory response was a two-fold increase in the standard deviation over the pre-stimulus period, plus the mean number of spikes, for at least three consecutive bins. The amplitude of excitatory responses was quantified by calculating the difference between the mean number of spikes evoked within the time window of the excitation and the mean number of spikes occurring spontaneously before the stimulation. The duration of an inhibitory response corresponded to the time interval during which no spikes were observed for at least three consecutive bins.

To better describe information transmission through these circuits, we set latency ranges for each pathway based on the latencies of triphasic responses, since these inform of the transmission through the three pathways that constitute the circuits. Such ranges were set up to each cortically-evoked response (i.e. early excitation, EE; inhibition, INH, late excitation, LE), in each circuit (i.e. SM or mPF) and experimental group (i.e. sham or 6-OHDA). For each response, a range was set according to the minimum and maximum latency observed within the triphasic-respondent neurons of that circuit and experimental group (Table S2). Hence, cortically evoked responses whose latency was out of this range were excluded from the analyses of the cortically evoked responses, and neurons with no cortically evoked response within range were excluded from all the analysis (cortically evoked and spontaneous firing parameters).

As more than one neuron (1–15 per rat) was recorded per animal in the characterization of the SM and mPF circuits, electrophysiological parameters such as firing rate, coefficient of variation, and parameters related to cortically evoked responses (i.e. duration, latency and amplitude of the responses) were averaged per animal, so that every animal had one value for each electrophysiological parameter.

2.6. Tyrosine hydroxylase immunohistochemistry

Immediately after the electrophysiological procedure, animals were transcardially perfused with a phosphate-buffered saline solution followed by 4% paraformaldehyde solution. Fixed brains were sliced at 40 μm by a freezing microtome (HM 430, Microm) and stored in a cryoprotective solution at −20 °C until further processing. Tyrosine hydroxylase (TH)-immunostaining was used to examine the degree of DA denervation in the striatum and the SNc as previously described (Aristieta et al., 2019, 2016). Free-floating sections were incubated in a 3% H_2O_2 + 10% MeOH solution prepared in potassium phosphate buffer saline with 0.1% Triton X-100 (KPBS-t) for 30 min. After that, sections were washed in KPBS and blocked with 5% normal goat serum (NGS) in KPBS-t during 1 h, and incubated with rabbit anti-TH (AB 152, 1:1000, Merck) primary antibody in 5% NGS-KPBS-t, at room temperature overnight. The sections were then washed in 2.5% NGS-KPBS-t, and incubated for 2 h with a biotinylated goat antibody against rabbit IgG (BA 1000, 1:200, Vector Laboratories) in 2.5% NGS-KPBS-t. Thereafter, sections were washed and incubated with an avidin–biotin–peroxidase complex (ABC kit, PK-6100, Vector Laboratories) and peroxidase activity was visualized with 0.05% 3,3′-diaminobenzidine (Sigma) and 0.03% H_2O_2. Finally, sections were mounted onto gelatin-coated slides, dehydrated, cleared with xylene and coverslipped. For the analysis, striatal sections from each animal (rostral, medial and caudal levels) were optically digitized using an EPSON V700 scanner at a resolution of 6400 ppp, and the mean optical density (OD) associated with the striatum was calculated using NIH-produced image analysis software ImageJ (Schindelin et al., 2012). The OD was expressed as a percentage of that of the contralateral intact side (100%) with the background associated with the corpus callosum set as 0%. Only animals with >90% DA degeneration were included in the analysis. Breakdown of these data into the different experimental groups is found in Table S1 and illustrated in the Fig. 1B.

2.7. CB1 receptor immunohistochemistry

Another series of animals (sham and 6-OHDA lesioned rats) were used to determine the expression of CB1 receptors within the BG. Rats were transcardially perfused with a phosphate-buffered saline solution followed by a mixture of 4% paraformaldehyde and 0.5% glutaraldehyde with 2 ml per litre of a saturated solution of picric acid in 0.1 M phosphate buffer (PB; pH 7.4). Brains were extracted and stored in fixative solution for one week. After fixation, brains were coronally cut at 50 μm by a cryotome.

Sections were preincubated in blocking solution containing 10% bovine serum albumin, 0.5% Triton X-100 and 0.1% sodium azide in Tris-HCl-buffered saline (TBS) for 30 min and then incubated in solution of primary goat antibody raised against CB1 cannabinoid receptor (CB1-Go-Af450 Frontier Institute Co.; RRID AB_257130) at a final dilution of

2 μg/ml in 10% bovine serum albumin, 0.5% Triton X-100 and 0.1% sodium azide in TBS for 20 h. Afterwards, sections were rinsed in 1% bovine serum albumin and 0.5% Triton X-100 in TBS and incubated in biotinylated horse-anti-goat secondary antibody (Vector BA-9500) diluted 15 μg/ml in 1% bovine serum albumin and 0.5% Triton X-100 in tris buffered saline for 1 h. After secondary antibody incubation, sections were again rinsed in 1% bovine serum albumin and 0.5% Triton X-100 in TBS saline and reacted for 90 min in ABC complex diluted 1:1:50 in TBS. After several rinses in PB, the peroxidase reaction with 0.05% DAB and 0.003% H_2O_2 in PB was developed for 2 min. Sections were rinsed in PB, mounted onto gelatine-coated microscope slides, allowed to air dry, dehydrated in graded ethanol, cleared in xylene and coverslipped. Microscope slides with the reacted tissue were scanned with the 20× objective (NA 0.8; Carl-Zeiss) of a Pannoramic MIDI II (3DHISTECH) automatic slide scanner coupled to a CMOS camera (pco. edge 4.2, PCO), through an adapter with 1.6× magnification. Images were studied with FIJI software using the Bio-Formats plugin (Linkert et al., 2010; Schindelin et al., 2012).

For the analysis of the CB1 receptor density we defined the regions of interest (ROI) for each anatomo-functional division in each nucleus based on previous tracing, molecular and functional reports, in which compartmentalization of the analysed BG nuclei is made depending on the cortical information they process. Regarding cortex, we focused on the MC and the ACC since they were the target of cortical stimulation in electrophysiological experiments. BG nuclei receiving information from MC were considered to belong to the SM circuits, and those receiving ACC information to the mPF circuits of the BG. MC and ACC ROI's were made following a rat brain atlas (Paxinos and Watson, 2006). Cortical areas were analysed until 0.4 mm posterior to bregma, where they were considered small enough to be properly selected. Striatal SM and mPF territories were limited to those areas receiving afferences from MC and ACC, respectively (Heilbronner et al., 2016; McGeorge and Faull, 1989). Globus pallidus SM and mPF territories were defined based on calbindin expression patterns, which resembles SM and mPF striatal projections onto the *globus pallidus* (Rajakumar et al., 1994). SM-SNr and mPF-SNr territories were defined based on functional studies showing connectivity between motor or mPF cortices, respectively (Kolomiets et al., 2003). For frontal slices the olfactory tract, forceps minor or corpus callosum, were selected as background. For more caudal slices, the thalamus, geniculate nucleus or reticular formation, were used as background.

To analyze changes in CB1 receptor density between lesion group (sham vs. 6-OHDA) and territories (SM or mPF) of the analysed BG nuclei, background OD from each hemisphere was subtracted from ROI's OD's in their corresponding hemisphere. Then values from both hemispheres of the same slice, corresponding to a given nucleus and territory, were averaged between them; averaged values from all the slices in an animal were averaged, so each animal would have two values per nucleus: one value for the SM territory, and another for the mPF territory. These values corresponding to the same BG territory and nucleus were averaged by lesion group.

2.8. Statistical analysis of data

The data were analysed using the computer program GraphPad Prism (v. 5.01, GraphPad Software, Inc.) and SPSS (v. 25; IBM Corp.). Averages from each rat for firing rate, CV and parameters related to cortically evoked responses were analysed by a two-tailed unpaired Student's *t*-test when looking for differences between sham and 6-OHDA-lesioned animals in both circuits. Fisher's exact test was used to assess differences in the number of neurons presenting bursting patterns and cortically evoked patterns of response.

To assess the effects of WIN 55,212-2 on firing rate, CV and parameters related to cortically evoked responses before and after drug application (one neuron per animal), a repeated-measures two-way ANOVA was used. When allowable, Bonferroni *post-hoc* method was used for correction of multiple comparisons. Fisher's exact test was used to assess differences in the number of neurons with burst firing before and after drug administration.

To determine the role of the CB1 receptor in the effect of WIN 55,212-2, the firing rate, CV, and cortically evoked responses pre-AM251, post-AM251 and post-AM251 + WIN 55,212-2, were compared using a repeated-measures one-way ANOVA in the SM circuits, and repeated-measures two-way ANOVA in the mPF circuits (one neuron per animal), both with Geisser-Greenhouse's correction if epsilon was below 0.75. When allowable, Bonferroni *post-hoc* method was used for correction of multiple comparisons. Differences in the number of neurons with burst firing were assessed with the chi-squared test.

CB1 receptor density averages from sham or 6-OHDA rats were compared using a two-way ANOVA (lesion × territory) to assess differences in CB1 receptor density between territories (SM and mPF) and lesion groups (sham and 6-OHDA). When allowable, Bonferroni *post-hoc* method was used for correction of multiple comparisons.

To assess differences in TH OD and ipsilateral forelimb use between sham and 6-OHDA rats a two-tailed unpaired Student's *t*-test was used.

The level of statistical significance was set at $P < 0.05$. Data are presented as group means ± the standard error of the mean (S.E.M.) of n rats, unless stated otherwise.

3. Results

3.1. Effect of dopaminergic denervation on SNr neuron activity from sensorimotor and prefrontal territories

All recorded cells exhibited the typical electrophysiological characteristics of GABAergic SNr neurons, including a narrow spike waveform and a relatively high firing rate (>7 Hz) with a regular pattern of discharge and response to cortical stimulation.

As summarized in Table 1, DA denervation differently affected SM-SNr and mPF-SNr neurons: the mean firing rate of mPF-SNr neurons was reduced in 6-OHDA-lesioned animals, while the mean firing rate of SM-SNr neurons in 6-OHDA-lesioned animals was not affected when compared to that of sham rats. Moreover, SM- and mPF-SNr neurons from lesioned animals presented a higher coefficient of variation than those from sham animals. In addition, the analysis of the firing pattern revealed that the number of neurons with bursts was increased in both SNr territories of the 6-OHDA-lesioned group.

As we previously showed, cortical stimulation of the MC or ACC evoked characteristic triphasic responses in SNr neurons that consisted of an early excitation followed by an inhibition and a late excitation (Antonazzo et al., 2019) (Fig. 1A). The presence of the early excitation is attributable to the activation of the so-called 'hyperdirect' cortico-subthalamo-nigral pathway. The activation of the 'direct' cortico-striato-nigral pathway give rise to the inhibition, and the late excitation derives from the activation of the 'indirect' cortico-striato-pallido-subthalamo-nigral pathway (Maurice et al., 1999). Different patterns of response can be observed in both SNr territories, yielding triphasic, biphasic or monophasic cortically evoked responses from the activation of the different pathways along the circuits. DA denervation induced changes in the percentage of neurons displaying different patterns of response in the SM-SNr territory (Table 2): the proportion of neurons displaying triphasic and biphasic (i.e., inhibition + late excitation) responses in SM-SNr neurons was reduced, in favour of more monophasic (i.e., early excitation) responses in the 6-OHDA-lesioned group. DA loss also altered patterns of response in mPF-SNr neurons, showing a greater amount of monophasic – inhibition – responses (Table 2). Overall, SM-SNr neurons displayed fewer inhibitions and late excitations, while the mPF-SNr neurons displayed only fewer late excitations after DA loss (Table 2).

DA denervation also affected the electrophysiological characteristics of cortically evoked responses in SNr neurons (Table 1). SM-SNr cells

Table 1
Electrophysiological characteristics of the spontaneous and cortically-evoked responses in neurons from the sensorimotor (SM) and medial prefrontal (mPF) subdivisions of the *substantia nigra pars reticulata* (SNr) in sham and 6-OHDA-lesioned rats.

	SM-SNr		mPF-SNr	
	Sham (n = 21)	6-OHDA (n = 36)	Sham (n = 32)	6-OHDA (n = 41)
Firing rate (Hz)	21.2 ± 1.8	19.0 ± 1.2	24.8 ± 1.3	19.4 ± 1.0*
Coefficient of variation (%)	43.6 ± 2.4	70.3 ± 4.6*	49.0 ± 2.4	102.5 ± 5.9*
Burst firing neurons/ recorded neurons	51/98	91/115	126/187	144/160
Neurons exhibiting burst firing pattern (%)	52.0	79.1*	67.4	89.6*
Early excitation	n = 19	n = 27	n = 30	n = 28
Duration (ms)	5.3 ± 0.4	8.3 ± 1.0*	7.2 ± 0.7	6.4 ± 1.0
Latency (ms)	5.5 ± 0.4	5.7 ± 0.3	8.5 ± 0.6	13.7 ± 0.5*
Amplitude	14.4 ± 1.3	13.2 ± 0.8	8.2 ± 0.5	7.9 ± 0.8
Inhibition	n = 20	n = 29	n = 32	n = 38
Duration (ms)	19.8 ± 2.1	27.6 ± 4.6	11.5 ± 0.8	13.0 ± 1.7
Latency (ms)	12.1 ± 0.4	14.0 ± 0.4*	18.8 ± 0.4	20.8 ± 0.4*
Late excitation	n = 21	n = 29	n = 32	n = 38
Duration (ms)	6.0 ± 0.5	7.5 ± 0.7	11.2 ± 0.8	11.3 ± 0.9
Latency (ms)	27.1 ± 0.6	27.7 ± 0.7	33.4 ± 0.4	33.5 ± 0.5
Amplitude	17.9 ± 2.5	13.7 ± 1.5	15.4 ± 1.0	13.8 ± 0.8

Each value represents the mean ± S.E.M. of (n) recorded rats.
* $P < 0.05$ Sham vs. 6-OHDA (Firing rate, coefficient of variation and response parameters: two-tailed unpaired Student's *t*-test; neurons exhibiting burst firing pattern: Fisher's exact test).

Table 2
Percentage of occurrence the different patterns of responses evoked in *substantia nigra pars reticulata* (SNr) neurons by motor or medial prefrontal cortex stimulation in sham and 6-OHDA-lesioned animals.

	SM-SNr		mPF-SNr	
	Sham (n = 98)	6-OHDA (n = 115)	Sham (n = 187)	6-OHDA (n = 160)
Total no. neurons showing early excitation (%)	60.2	66.1	30.5	28.1
Total no. neurons showing inhibition (%)	75.5	51.3*	65.8	70.6
Total no. neurons showing late excitation (%)	65.3	46.1*	86.1	70.6*
Patterns of responses (%)				
Triphasic response	29.6	16.5*	19.8	11.9
Early excitation + Inhibition	21.4	22.6	3.2	5
Inhibition + Late excitation	16.3	3.5*	38	36.9
Early excitation + Late excitation	4.1	4.3	1.6	3.8
Early excitation	5.1	22.6*	5.9	7.5
Inhibition	8.2	8.7	4.8	16.9*
Late excitation	15.3	21.7	26.7	18.1

Each value represents the number of neurons exhibiting the response to cortical stimulation (% of n recorded neurons).
* $P < 0.05$ vs sham, Fisher's exact test.

from 6-OHDA-lesioned animals had early excitations with greater durations than those recorded from sham rats. In the case of mPF-SNr neurons, DA denervation increased the latency of the early excitation. Moreover, the inhibition appeared later in the SM- and mPF-SNr neurons of 6-OHDA-lesioned animals, as indicated by a higher latency. It is important to note that, when only triphasic responses were taken into account, only the differences in mPF-SNr neurons remained, while no differences in electrophysiological characteristics were found in SM-SNr neurons between groups (Table S2).

3.2. Effects of WIN 55,212-2 on cortico-nigral transmission through the sensorimotor circuits in sham and 6-OHDA-lesioned rats

The effect of the synthetic cannabinoid agonist WIN 55,212-2 (WIN) (125 μg/kg, i.v.) on the transfer of cortical information through the SM circuits in intact and 6-OHDA-lesioned rats was investigated. The dose of WIN was carefully selected to minimize any effects on the firing activity of SNr neurons, which could make the analysis of the cortically-evoked responses difficult. Thus, at the administered dose, WIN did not modify the SM-SNr neuron firing rate or the number of neurons with burst activity in the sham and 6-OHDA experimental groups, although some minor changes were observed regarding the regularity (Table S3).

According to our previous data (Antonazzo et al., 2019), in sham rats, systemic administration of WIN did not alter early excitation but diminished cortico-nigral transmission through the indirect pathway, as shown by a reduction in the amplitude of the late excitation. However, no statistically significant decrease was observed in the transmission through the direct pathway (Fig. 2). In contrast to that observed in the sham group, 6-OHDA lesions modified the effect of WIN on cortico-nigral transmission through the SM circuits, being the early excitation decreased after drug administration. However, cortico-nigral information transfer through the trans-striatal pathways was not affected after WIN administration in 6-OHDA-lesioned animals (Fig. 2).

The effects observed in sham rats were blocked by the previous administration of the CB1-selective antagonist AM251 (2 mg/kg, i.v.) (Fig. 3). AM251 alone did not modify the cortico-nigral information transfer (Fig. 3) or the spontaneous activity of SM-SNr neurons (Table S4).

3.3. Effects of WIN 55,212-2 on cortico-nigral transmission through the medial prefrontal circuits in sham and 6-OHDA-lesioned rats

We further explored the effect of WIN (125 μg/kg, i.v.) on cortico-nigral transmission through the mPF circuits in intact and 6-OHDA-lesioned rats. At the administered dose, WIN did not modify the mPF-SNr neuronal firing rate or the number of neurons displaying burst activity. Nevertheless, some minor changes were observed regarding regularity (Table S3).

As previously shown in control animals (Antonazzo et al., 2019), WIN administration dramatically impaired all cortically evoked responses, reducing the amplitude of the early and late excitations and the duration of the inhibition (Fig. 4). As in SM circuits, DA denervation induced changes in the way WIN modulates transmission through the mPF circuits. The administration of WIN reduced the amplitude of the early excitation but had no effect on cortical information transfer through the direct and indirect pathways (Fig. 4).

These effects were blocked by the previous administration of the CB1-selective antagonist AM251 (2 mg/kg, i.v.) in both sham and 6-OHDA-lesioned animals (Fig. 5). AM251 alone did not modify the cortico-nigral information transfer (Fig. 5) or the spontaneous activity of mPF-SNr neurons (Table S4).

3.4. CB1 receptor localization in the sensorimotor and prefrontal circuits of the basal ganglia in sham and 6-OHDA-lesioned rats

Finally, CB1 immunostaining was performed in all BG structures

included in the SM and mPF circuits. The study of the mean OD obtained from all the slices through each structure, and the comparison between the divisions related to the SM and mPF circuits for every nucleus sampled revealed some differences. In the striatum from sham animals, the CB1-positive labelling in the lateral division related to the SM circuit was higher than in the mPF-related division. This difference was also statistically significant in 6-OHDA-lesioned animals (Fig. 6).

On the other hand, no statistically significant changes were found in the CB1 receptor immunostaining between sham and 6-OHDA-lesioned rats, in any of the analysed territories of the BG nuclei (Fig. 7).

4. Discussion

In the present study, we investigated the functioning of BG circuits and their modulation by the CB1 receptor under DA-depleted conditions. The results show that the DA deficit modifies the transmission through the SM and mPF circuits. Moreover, we observed an alteration at the level of CB1 receptors modulating cortico-BG information transfer in 6-OHDA-lesioned animals. Given the role of these circuits in motor and cognitive/motivational information processing, the present data may help researchers to understand the role of the cannabinoid system in motor and non-motor symptoms associated with the hypodopaminergic state.

4.1. Spontaneous and cortically evoked SNr neuron activity after DA denervation

According to our data, in DA-depleted animals, SNr neurons recorded in the mPF and SM regions exhibited alterations in spontaneous activity, displaying more irregular and burst firing patterns (Aristieta et al., 2016; Vegas-Suárez et al., 2020). However, only in the mPF-SNr neurons did we observe a significant reduction in the firing rate. In line with our results, Wang et al. (2010) showed a decreased firing rate and an increased CV and burst activity in mPF-SNr neurons in animals injected with 6-OHDA in the MFB. Regarding the SM territory, there is much more evidence supporting the hyperactive SNr neuronal discharge pattern after DA depletion, without changes in the firing rate (Aristieta et al., 2016; Maurice et al., 2015; Meissner et al., 2006; Murer et al., 1997; Tseng et al., 2000). Several studies suggest that there might be a mediolateral gradient in DA content in the SNr, with less DA in the SM-SNr and more DA in the mPF-SNr (Ciliax et al., 1995; Cragg et al., 1997; Rice et al., 1994, 1997; Weiss-Wunder and Chesselet, 1990). This suggestion is in accordance with the greater effect of DA denervation observed on the firing rate and pattern of mPF-SNr neurons. Our data suggest that mPF-SNr neurons rely more on DA for their normal function than SM-SNr neurons. The effects of DA denervation on SNr spontaneous activity likely involve an indirect mechanism, like modulation of presynaptic GABAergic or glutamatergic inputs, since SNr neurons lack

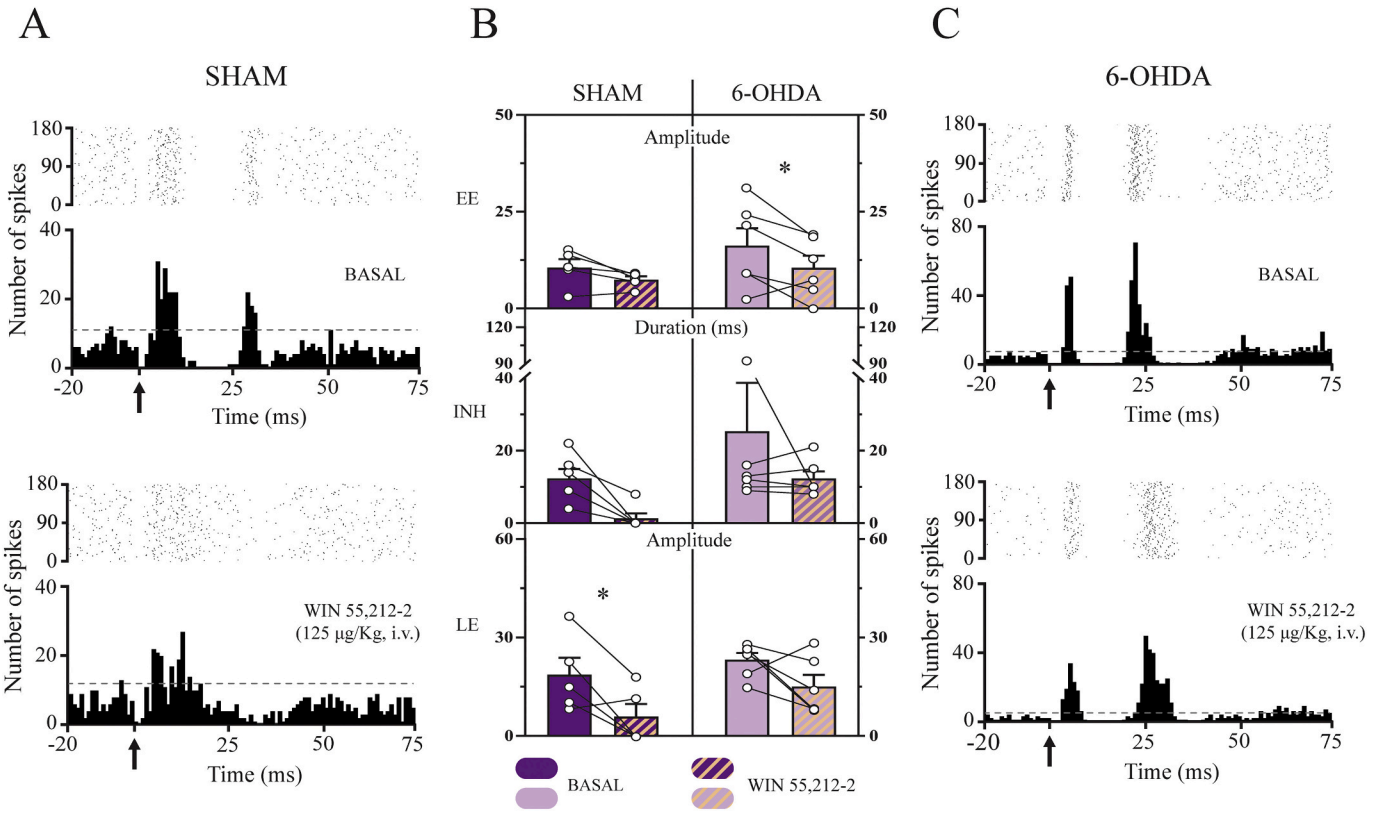

Fig. 2. Effect of systemic administration of WIN 55,212-2 (125 µg/kg, i.v.) on cortico-nigral information transmission in sensorimotor (SM) BG circuits in sham and 6-OHDA-lesioned animals.

A. Top, raster plot and peristimulus time histogram showing a representative example of a triphasic response evoked in an SM-SNr neuron from a sham rat through the stimulation of the motor cortex (MC) under basal conditions. Bottom, after WIN 55,212-2 injection, the inhibitory and late excitatory components disappeared, with the early excitation remaining unaltered. Arrows indicate cortical stimulus application. Dashed lines indicate the threshold for excitatory responses. C. Top, raster plot and peristimulus time histogram showing a representative example of a triphasic response evoked in an SM-SNr neuron from a 6-OHDA-lesioned animal through the stimulation of the motor cortex under basal conditions. Bottom, after WIN 55,212-2 injection, none of the three pathways experienced any change in transmission in 6-OHDA-denervated animals. Arrows indicate cortical stimulus application. Dashed lines indicate the threshold for excitatory responses. B. Bar graphs showing the mean effect of WIN 55,212-2 (125 µg/kg, i.v.) on cortically evoked responses in SM-SNr neurons (amplitude of early (EE; sham: n = 5; 6-OHDA: n = 6) and late (LE; sham: n = 5; 6-OHDA: n = 6) excitations and the duration of inhibition (INH; sham: n = 6; 6-OHDA: n = 6)) in SM circuits. Each bar represents the mean ± the S.E.M. of n rats. Each dot represents the value from one neuron before and after drug administration. *$P < 0.05$ before vs. after WIN, repeated-measures two-way ANOVA (Drug x Lesion).

postsynaptic DA receptors (Yung et al., 1995). According to the classical BG organization model, the direct striatonigral pathway is under the control of DA projections via D1 receptors, whereas the striato-pallido-subthalamo-nigral indirect pathway is controlled via D2 receptors. Degeneration of nigrostriatal DA neurons results in a dramatic decrease of striatal DA level and, subsequently, in a supersensitivity of the striatal postsynaptic DA receptors affecting the direct and indirect pathways and triggering SNr neuron activity abnormalities (Galvan and Wichmann, 2008). Thus, in line with our previous data, SNr neurons recorded in the mPF and SM regions from 6-OHDA lesioned animals displayed more irregular and burst firing patterns, probably related with the well described hyperactivated subthalamic nucleus after DA depletion. Moreover, in mPF-SNr neurons we observed a significant reduction in the firing rate that might be due to an increase in the number of D2 receptors in the limbic striatum after striatal DA depletion, which activation inhibits SNr neuronal firing via their intracellular effects on G_i proteins (Lévesque et al., 1995).

In relation to the SM circuit, we show a prominent transmission through the hyperdirect trans-subthalamic pathway reflected by a greater mean duration and more monophasic early excitations. These data differ, at least in part, from the evidence available to date, although the heterogeneous results may depend on methodological differences like the use of different anaesthetic regime (chloral hydrate, urethane or awake animals) (Beyeler et al., 2010; Heckman et al., 2018; Kolomiets et al., 2003; Maurice et al., 1999; Sano and Nambu, 2019), or dopaminergic interruption method (6-OHDA lesion or pharmacological blockade) (Degos et al., 2005; Sano and Nambu, 2019). Moreover, the degree of dopaminergic denervation, and time after the 6-OHDA injection, may also impact on results.

Degos et al. (2005) studied the effect of acute pharmacological blockade of DA transmission on circuit functionality, but by systemic injection of neuroleptics. They showed decreased transmission through the direct pathway and a reinforced transmission through the indirect pathway, without any change in the information transfer through the hyperdirect pathway. Using the 6-OHDA neurotoxin, other authors either have found no alterations (injected into the *substantia nigra pars compacta*) (Maurice et al., 2015) or have described early excitations as the predominant response after dopaminergic denervation (injected into the MFB, but recordings in awake mice) (Sano and Nambu, 2019). However, although this might be in accordance with our results, the authors also found an increase in transmission through the indirect pathway, concluding that only neuronal transduction through the direct pathway is diminished in PD. Predominant transmission through the hyperdirect pathway in the SM circuit observed in the present study, together with the hyperactivity of SM-SNr neurons, is consistent with the overactive state of the subthalamic nucleus extensively described under low DA conditions and has been related to the motor features of parkinsonism (Benabid et al., 1994; Bergman et al., 1994; Hassani et al., 1996; Steigerwald et al., 2008).

To our knowledge, the present is the first demonstration that DA denervation alters the cortically evoked responses in mPF-SNr neurons, leading to a predominant information transfer though the direct pathway, with a loss of efficacy in the transmission through the hyperdirect and indirect pathways (augmented latency of early excitations or

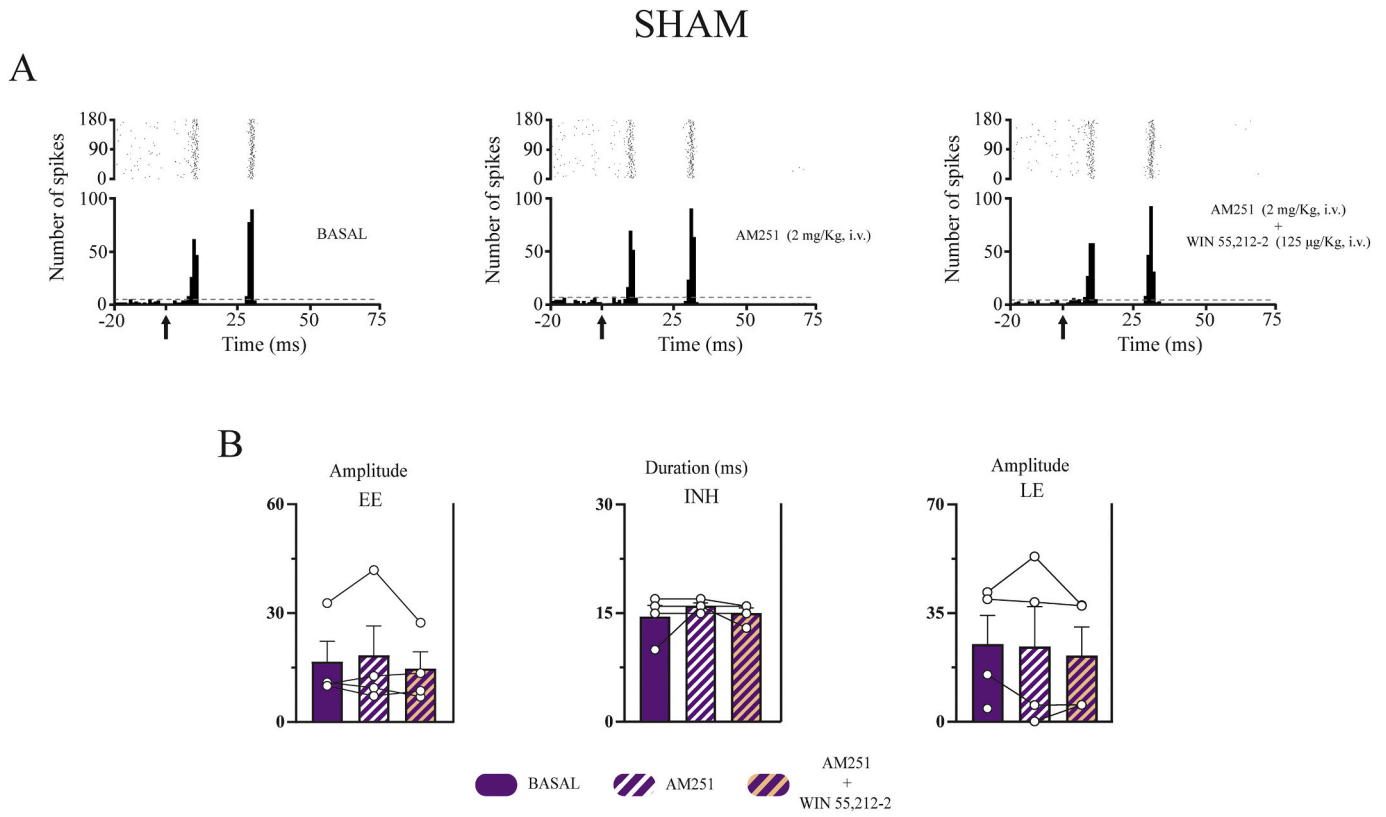

Fig. 3. Blockade of WIN 55,212-2-induced effects on cortico-nigral information transmission in sensorimotor (SM) BG circuits in sham animals by the previous administration of the CB1 selective antagonist AM251 (2 mg/kg, i.v.).

A. Left, raster plot and peristimulus time histogram showing a representative example of a triphasic response evoked in a SM-SNr neuron by stimulation of the motor cortex (MC) in a sham rat under basal conditions. AM251 administration did not modify the characteristics of the three components of the cortically evoked response (middle) but blocked the effects induced by WIN 55,212-2 (right). Arrows indicate cortical stimulus application. Dashed lines indicate threshold for excitatory responses. B. Bar graphs showing the mean effect of AM251 (2 mg/kg, i.v.) and WIN 55,212-2 (125 µg/kg, i.v.) on cortically evoked responses in SM-SNr neurons (amplitude of early (EE; n = 4) and late (LE; n = 4) excitations and duration of inhibition (INH; n = 4)) in SM circuits. Each bar represents the mean ± S.E.M. of n rats. Each dot represents the value from one neuron before and after drug administration.

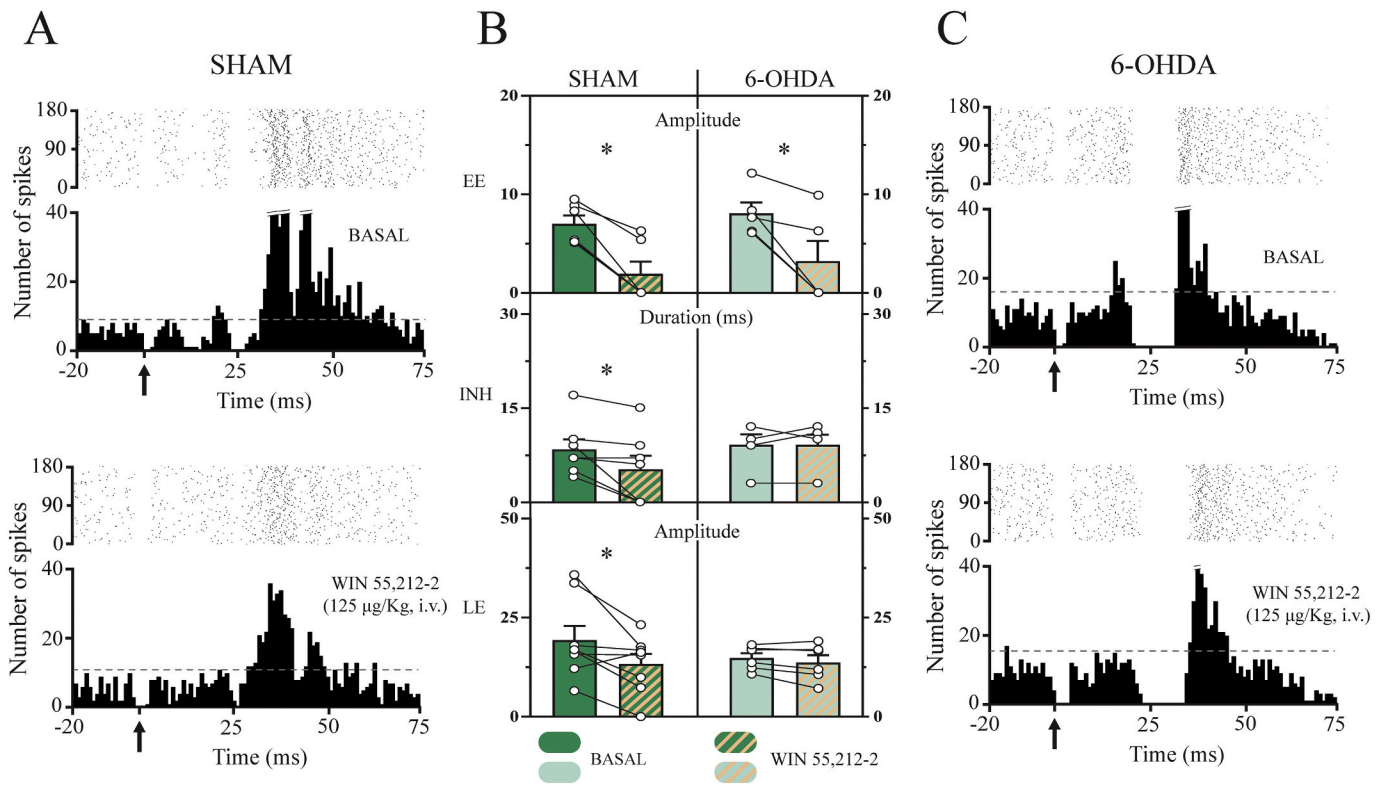

Fig. 4. Effect of systemic administration of WIN 55,212-2 (125 µg/kg, i.v.) on cortico-nigral information transmission in medial prefrontal (mPF) BG circuits in sham and 6-OHDA-lesioned animals.

A. Top, raster plot and peristimulus time histogram showing a representative example of a triphasic response evoked in an mPF-SNr neuron from a sham rat through the stimulation of the anterior cingulate cortex (ACC) under basal conditions. Bottom, WIN 55,212-2 injection was able to reduce transmission through the three pathways. Arrows indicate cortical stimulus application. Dashed lines indicate the threshold for excitatory responses. C. Top, raster plot and peristimulus time histogram showing a representative example of a triphasic response evoked in an mPF-SNr neuron from a 6-OHDA-lesioned animal through the stimulation of the ACC under basal conditions. Bottom, after WIN 55,212-2 injection, only reduced transmission of the early excitation in 6-OHDA-denervated animals was observed. Arrows indicate cortical stimulus application. Dashed lines indicate the threshold for excitatory responses. B. Bar graphs showing the mean effect of WIN 55,212-2 (125 µg/kg, i.v.) on cortically evoked responses in mPF-SNr neurons (amplitude of early (EE; sham: n = 6; 6-OHDA: n = 5) and late (LE; sham: n = 8; 6-OHDA: n = 6) excitations and the duration of inhibition (INH; sham: n = 7; 6-OHDA: n = 5)) in mPF circuits. Each bar represents the mean ± the S.E.M. of n rats. Each dot represents the value from one neuron before and after drug administration. $^{*}P < 0.05$ before vs. after WIN, repeated-measures two-way ANOVA (Drug x Lesion).

less late excitations). These data, together with the important modifications of the spontaneous activity of mPF-SNr neurons, indicate abnormal functionality inside associative and limbic territories of the BG. In fact, behavioural studies performed in similar PD models show cognitive dysfunctions, such as apathy (Anderson et al., 2020; Carvalho et al., 2013; Furlanetti et al., 2015) or depression-like behaviours (Winter et al., 2007; Zhang et al., 2011), that are linked to the BG and are present in PD patients (Tremblay et al., 2015). Thus, the alterations observed in this study in the mPF circuits after DA denervation might help understand the neurobiological components behind these motivational symptoms in PD patients.

Overall, our results indicate that DA depletion along with probable compensatory changes induced by DA denervation itself, lead to deficits in cortical information selection through the segregated anatomo-functional cortico-BG loops. In the mPF circuits, the information through the direct pathway is enhanced, while in the SM circuits, the enhancement takes place in the hyperdirect pathway. Although, in principle, these data would not be in line with studies showing striatal medium spiny neurons (MSN) hyperactivation (both those expressing D1 (dMSN) and those expressing D2 receptors (iMSN)) in animal models and PD patients (Fieblinger et al., 2014; Singh et al., 2016; Suarez et al., 2016), other factors could influence the output of the circuits seen in SNr neurons after cortical stimulation. Some studies point out alterations during hypodopaminergic states such as dendritic atrophy, spine pruning and reduced corticostriatal glutamatergic synapses in dMSN, iMSN or both MSN's that could be reducing cortical input on these neurons (Fieblinger et al., 2014; Gagnon et al., 2017; Graves and Surmeier, 2019; Suarez et al., 2016). Moreover, functional studies show a decreased corticostriatal connectivity in dMSN's, and increased in iMSN's in a 6-OHDA model similar to ours, in line with the classical model of BG function in hypodopaminergic states (Escande et al., 2016; Mallet et al., 2006). Overall, this evidence would support the reduced percentage of neurons displaying direct pathway activation (inhibitory component of the cortically-evoked response in SNr neurons) that we observe in the SM circuits of 6-OHDA animals. However, the reduced transmission through the indirect pathway of the SM circuits in lesioned group is contradictory. Being the indirect pathway a polysynaptic pathway, interpretation of the effects of DA denervation grows in complexity, especially if we consider the impact of the DA loss in pallidal and subthalamic function (Chan et al., 2011; Magill et al., 2001; Miguelez et al., 2012). Moreover, one characteristic of the BG nuclei is the high synaptic convergence in its output nuclei. Mallet et al. (2006) showed that DA denervation increases the time window in which iMSN's respond to stimulation of the MC. This variability in the response time of iMSN's after cortical stimulation could make the summation of multiple inputs on neurons in downstream nuclei difficult, failing to engage neuronal activity efficiently, and provoke full transmission through the indirect pathway, reaching the SNr.

Regarding the mPF circuits, we observed only a decrease in the number of neurons showing a late excitation, related with decreased indirect pathway activation. Most of the studies discussed above address how BG physiology is altered in hypodopaminergic states with special

emphasis on the SM territories, but few have addressed this same topic on the mPF territories of the BG. Some studies manifest substantial differences between SM and mPF territories. For instance, sensory- and limbic-related cortical areas preferentially innervate dMSN's, whilst motor-related areas innervate iMSN's (Wall et al., 2013). Moreover, functional studies have shown different forms of plasticity taking place under different conditions in SM and mPF territories of the striatum, besides differences in components from key striatal neurotransmitter systems (Arbuthnott and Wickens, 2007; Atwood et al., 2014; Braz et al., 2017; Herkenham et al., 1991). Together, this evidence calls for caution in extrapolating traits related with components from the SM circuits, into components from the mPF circuits. These differences could affect the way mPF circuits behaves, not only under physiological conditions, but also in pathological states, therefore stepping aside from what is expected from BG physiology under DA denervation.

The abnormal selectivity of information affecting motor, cognitive and motivational domains could be the neurophysiological impetus to the development of the motor and non-motor symptoms observed in PD, and it can be due to reduced anatomical and functional connectivity in cortico-BG networks, as demonstrated in PD patients and more evident for SM connections (Sharman et al., 2013).

4.2. *Dysfunctional CB1-mediated modulation of cortico-BG information transmission*

CB1-mediated modulation of cortical information transmission through the SM or mPF BG circuits is changed in 6-OHDA-lesioned animals. In agreement with our previous work in control animals (Antonazzo et al., 2019), administration of WIN in sham rats caused a reduction in the information transmission through the indirect pathway, without affecting the hyperdirect pathway in the SM circuits. Regarding the mPF circuits, administration of WIN in sham rats decreased information transmission through the three pathways. However, no statistically significant reduction of the transmission through the direct pathway was observed in this study in the SM circuits, in contrast to our previous work in control animals. This could be due to the extreme value present in the 6-OHDA dataset, which could likely be introducing noise, therefore confusing the statistical test. In support of this, data obtained here and in our previous work (Antonazzo et al., 2019) before and after WIN administration is similar, both mean and dispersion values (Before WIN: 12.3 ± 2.6 vs. 15.0 ± 1.5; After WIN: 3.5 ± 2.3 vs. 4.4 ± 2.1).

After dopaminergic denervation, the hyperdirect pathway in the SM circuits became sensitive to WIN administration. Previous work in our lab shows that administration of WIN in 6-OHDA-lesioned rats reduces

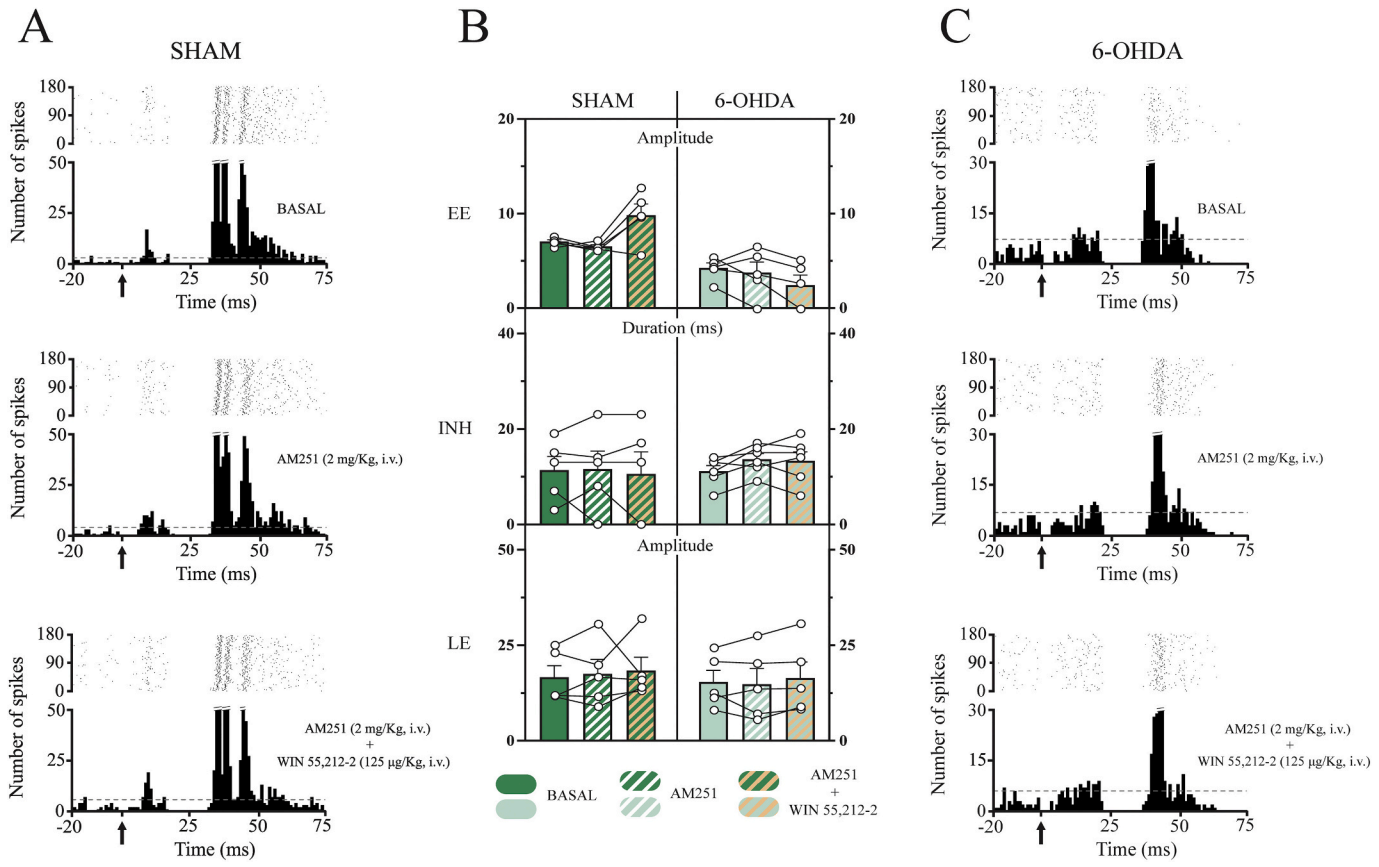

Fig. 5. Blockade of WIN 55,212-2-induced effects on cortico-nigral information transmission in medial prefrontal (mPF) BG circuits in sham and 6-OHDA-lesioned animals by the previous administration of the CB1 selective antagonist AM251 (2 mg/kg, i.v.).
A. Top, raster plot and peristimulus time histogram showing a representative example of a triphasic response evoked in a mPF-SNr neuron by stimulation of the anterior cingulate cortex (ACC) in a sham rat under basal conditions. AM251 administration did not modify the characteristics of the three components of the cortically evoked response (middle) but blocked the effects induced by WIN 55,212-2 (bottom). Arrows indicate cortical stimulus application. Dashed lines indicate threshold for excitatory responses. C. Top, raster plot and peristimulus time histogram showing a representative example of a triphasic response evoked in a mPF-SNr neuron by stimulation of the ACC in a 6-OHDA rat under basal conditions. AM251 administration did not modify the characteristics of the three components of the cortically evoked response (middle) but blocked the effects induced by WIN 55,212-2 (bottom). Arrows indicate cortical stimulus application. Dashed lines indicate threshold for excitatory responses. B. Bar graphs showing the mean effect of AM251 (2 mg/kg, i.v.) and WIN 55,212-2 (125 µg/kg, i.v.) on cortically evoked responses in mPF-SNr neurons (amplitude of early (EE; sham: n = 5; 6-OHDA: n = 5) and late (LE; sham: n = 5; 6-OHDA: n = 5) excitations and duration of inhibition (INH; sham: n = 5; 6-OHDA: n = 6) in mPF circuits. Each bar represents the mean ± S.E.M. of n rats. Each dot represents the value from one neuron before and after drug administration.

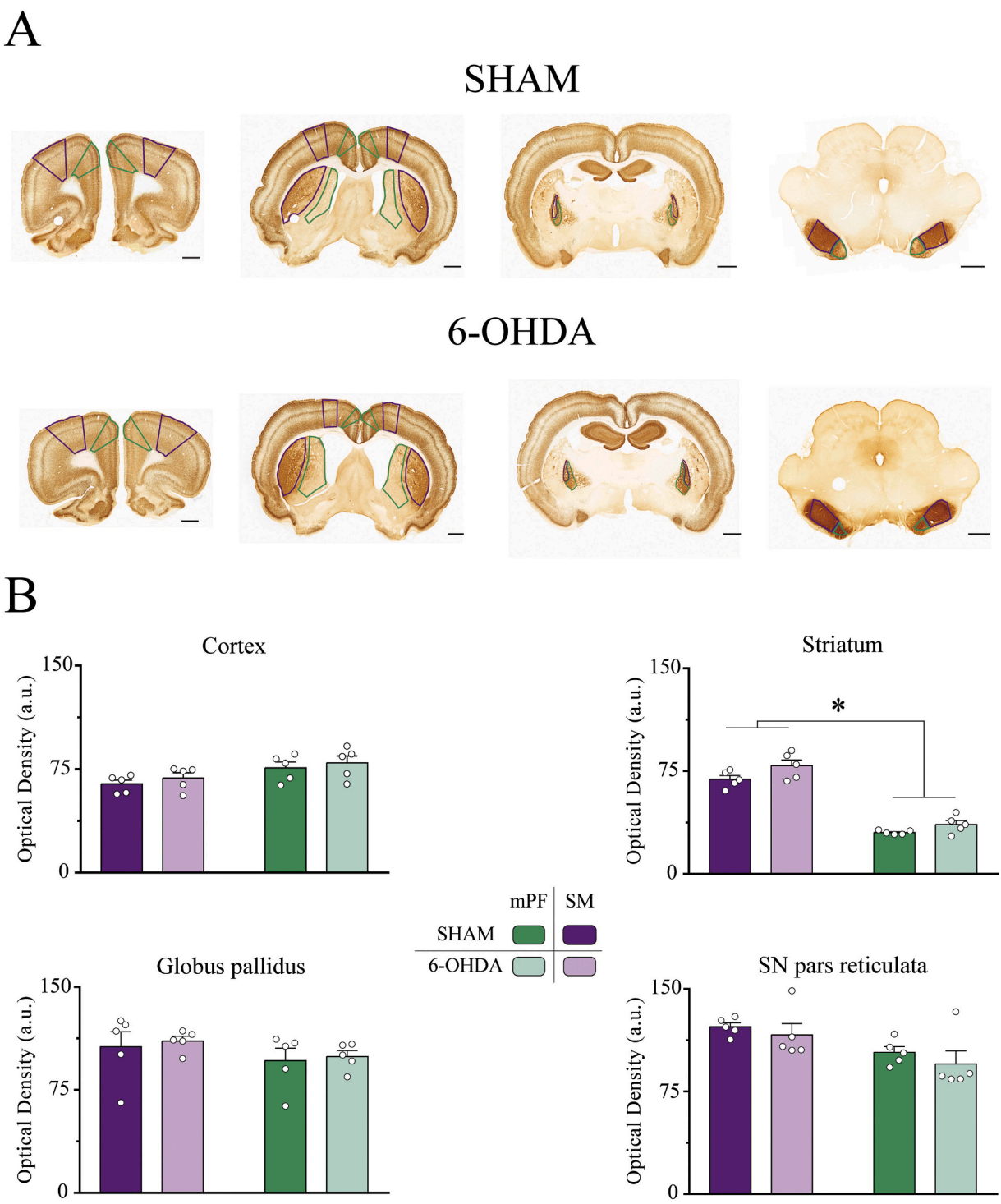

Fig. 6. CB1 receptor immunoreactivity in the sensorimotor (SM) and medial prefrontal (mPF) basal ganglia territories in the cortex, striatum, globus pallidus and substantia nigra pars reticulate from sham and 6-OHDA-lesioned rats.

A. Representative sham rat (top) and 6-OHDA-lesioned (bottom) rats brain slices showing CB1 receptor immunoreactivity in the studied areas. SM and mPF analysed territories are marked in purple and green, respectively. B. Bar graphs showing the mean CB1 receptor optical density (OD) in the SM and mPF territories of the studied brain areas in sham and 6-OHDA-lesioned animals. Note that there is significantly less CB1 receptor immunoreactivity in the mPF territories of the striatum in both sham and 6-OHDA-lesioned animals compared to SM territories. Scale bars are set to 1 mm. Each bar represents the mean ± the S.E.M. of n rats. Each dot represents the averaged value from one rat. *$P < 0.05$ SM vs. mPF, repeated-measures two-way ANOVA (Territory × Lesion). (For interpretation of the references to colour in this figure legend, the reader is referred to the web version of this article.)

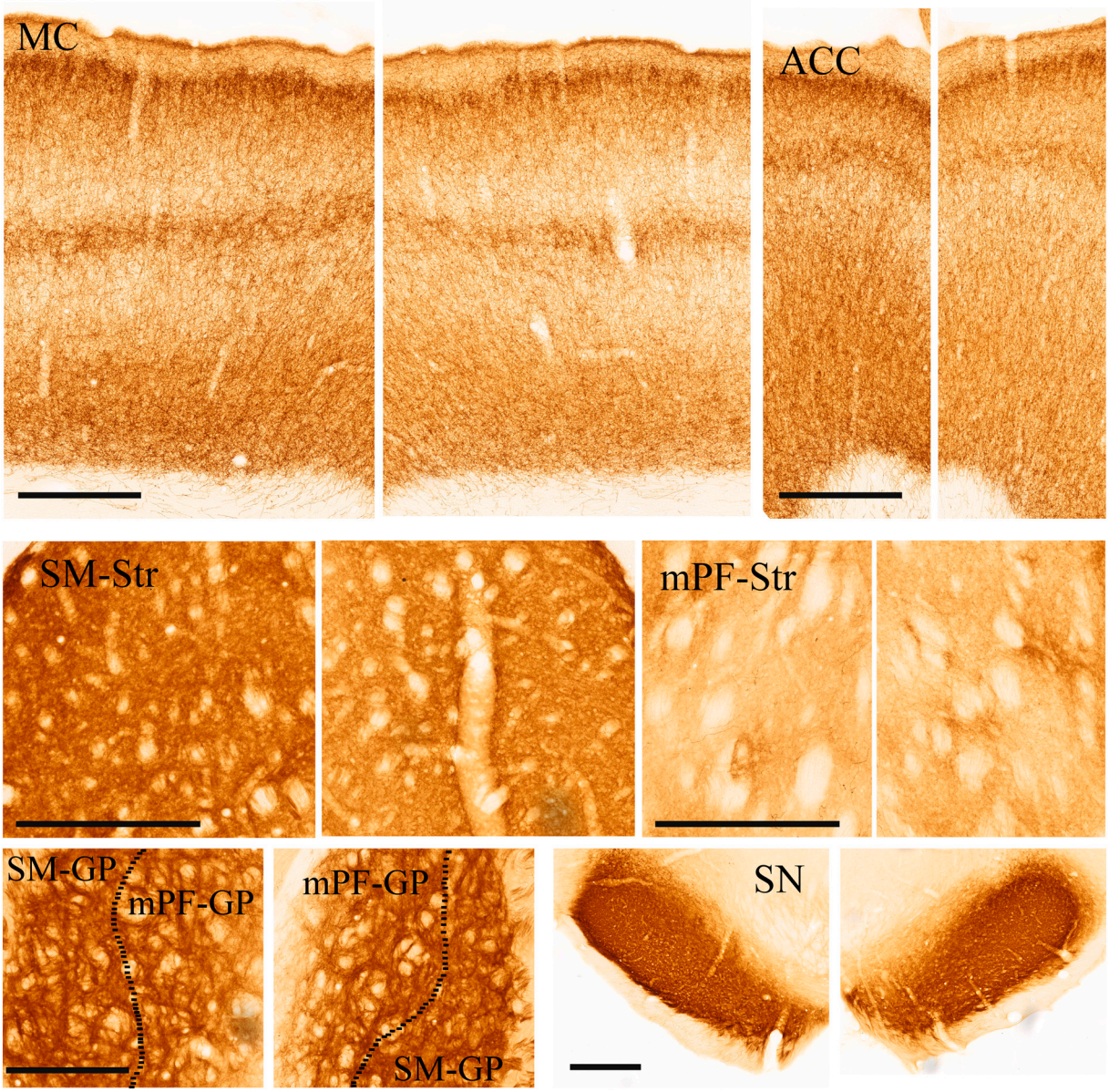

Fig. 7. Regional distribution of CB1 receptor expression in the basal ganglia nuclei from 6-OHDA-lesioned rats.
Brain microphotographs of coronal sections showing the CB1 receptor immunohistochemistry. The first row shows the distribution of the CB1 receptor in the motor cortex (MC) and anterior cingulate cortex (ACC). Second row shows the sensorimotor territory (dorsolateral striatum; SM-Str) and the medial prefrontal territory (dorsomedial striatum; mPF-Str). Third row shows the globus pallidus divided in its sensorimotor (SM-GP) and medial prefrontal territory (mPF-GP), and the susbstantia nigra (SN). Studied areas are shown in pairs, being the pictures on the left from the lesioned hemisphere. Scale bars are set to 500 μm.

firing rate of subthalamic nucleus neurons (Morera-Herreras et al., 2011), which could explain the reduced transmission through the hyperdirect pathway after WIN administration in these circuits. In the mPF circuits, this pathway remains sensitive to WIN in the 6-OHDA group. However, trans-striatal pathways in both circuits became insensitive to WIN after DA denervation.

A possible explanation for the observed findings could be the alteration of CB1 receptor expression induced by DA depletion. For this reason, we decided to perform immunohistochemical assays to determine the precise territory-specific potential changes in each nucleus conforming the BG circuits. In sham animals, sub-territorial immunolabelling analysis revealed predominant CB1 expression in the SM areas of the striatum compared to associative/limbic striatal regions. These data is consistent with previous work reported by other authors (A. G. Hohmann and Herkenham, 1999; Mailleux and Vanderhaeghen, 1992; Marsicano and Lutz, 1999; Matsuda et al., 1993; Van Waes et al., 2012; Zimmer et al., 1999), overall suggesting that CB1 receptors located in these anatomical regions of the BG could predominantly regulate SM information processing, or at least to a greater extent than mPF receptors. In the SM areas of the striatum, and given the preferential location of the CB1 receptor on terminals (Irving et al., 2000), extensive location of the CB1 receptor in SM territories likely comes from MSN's axon collaterals. Therefore, contributions from striatal afferents to CB1 immunostaining in SM territories is probably minimal. Although the CB1 receptor is expressed in cortical areas projecting to SM territories of the striatum, this expression is modest, and located principally in non-pyramidal neurons (Heng et al., 2011; Mailleux and Vanderhaeghen, 1992). Moreover, midbrain dopaminergic neurons and thalamic neurons show negligible levels of CB1 expression (Herkenham et al., 1991; Mailleux and Vanderhaeghen, 1992). This is in line with the sparse CB1 presence in mPF territories of the striatum, where the expression of this receptor is also minimal (Hohmann and Herkenham, 2000; Van Waes

et al., 2012). In this case, sparse CB1 immunostaining would likely come from afferences like mPF cortical areas, and to some extent hippocampus and amygdala where CB1 receptor is highly expressed (Herkenham et al., 1991; Mailleux and Vanderhaeghen, 1992; Voorn et al., 2004). Overall, contribution to CB1 immunostaining from striatal interneurons is probably low since they represent <3% of the total number of striatal neurons, regardless that some of them express CB1 receptor (Hohmann and Herkenham, 2000; Martín et al., 2008; Oorschot et al., 2002).

Additionally, we did not find any topographical difference in CB1 receptor expression under conditions of low DA, although the higher CB1 expression in the striatal SM area was preserved compared to the mPF. In agreement with our observations, using the unilateral-MFB 6-OHDA rat model, no changes in CB1 receptor binding in the BG have been described, measured by [^{3}H]-WIN-55,212-2 autoradiography 7–10 weeks after the lesion (Romero et al., 2000), by immunohistochemistry at different post-lesion time points (Walsh et al., 2010), or by mRNA in situ hybridization histochemistry (Zeng et al., 1999). More recently, similar results have been reported in MPTP parkinsonian monkeys (Rojo-Bustamante et al., 2018). Data coming from *post-mortem* brain tissue of PD patients are inconclusive, showing increased (Lastres-Becker et al., 2001) or no changes (Farkas et al., 2012) in CB1 receptor binding or decreased receptor expression measured through mRNA (Hurley et al., 2003).

Taking into account these results, we can conclude that, in our experimental conditions, CB1 receptor expression in BG nuclei is not affected by DA denervation, indicating that the loss of cannabinoid modulation of cortico-BG circuits could be due to a mechanism related to an alteration of CB1 receptor functionality. In this aspect, current evidence also shows some discrepancies, describing increased activation of GTP-binding proteins in PD patients treated with L-DOPA and MPTP marmosets (Lastres-Becker et al., 2001) as well as no changes in 6-OHDA-lesioned rats (Romero et al., 2000). In our experimental model, and according to the observed results, we hypothesize that after 4–5 weeks of DA depletion induced by unilateral-MFB 6-OHDA injection, CB1 receptor hyposensitivity occurs within the cortico-BG circuits, which could explain the lack of the modulation of these networks.

5. Conclusions

In summary, the present study allows us to better understand the non-motor functions of the BG and highlights not only dysfunctional motor information processing though the cortico-BG circuits but also abnormal information transfer through the associative/limbic domains after DA loss. This unusual mPF BG circuitry functionality could be related to the cognitive deficits and behavioural disorders that occur in PD. Therefore, the targeting of limbic/associative BG circuits and the restoration of CB1 functionality could constitute a promising target for the treatment of these non-motor symptoms manifested by PD patients.

Funding

This study was supported by grants from the Basque Government (PIBA 2019-38), the University of the Basque Country (GIU19/092), and the MINECO fund SAF2016-77758-R (AEI/FEDER, UE). M.A, has a fellowship from the MECD.

CRediT authorship contribution statement

Mario Antonazzo: Data curation, Formal analysis, Investigation, Visualization, Writing - original draft, Writing - review & editing. **Sonia María Gomez-Urquijo:** Investigation, Visualization, Writing - original draft, Writing - review & editing. **Luisa Ugedo:** Funding acquisition, Project administration, Supervision, Writing - original draft, Writing - review & editing. **Teresa Morera-Herreras:** Conceptualization, Funding acquisition, Project administration, Supervision, Writing - original draft, Writing - review & editing.

Declaration of Competing Interest

None.

Acknowledgments

We thank L. Escobar for her technical assistance with immunohistochemistry image acquisition.

Appendix A. Supplementary data

Supplementary data to this article can be found online at https://doi.org/10.1016/j.nbd.2020.105214.

References

Alexander, G.E., DeLong, M.R., Strick, P.L., 1986. Parallel organization of functionally segregated circuits linking basal ganglia and cortex. Annu. Rev. Neurosci. 9 (1), 357–381. https://doi.org/10.1146/annurev.ne.09.030186.002041.

Anderson, C., Sheppard, D., Dorval, A.D., 2020. Parkinsonism and subthalamic deep brain stimulation dysregulate behavioral motivation in a rodent model. Brain Res. 1736, 146776. https://doi.org/10.1016/j.brainres.2020.146776.

Antonazzo, M., Gutierrez-Ceballos, A., Bustinza, I., Ugedo, L., Morera-Herreras, T., 2019. Cannabinoids differentially modulate cortical information transmission through the sensorimotor or medial prefrontal basal ganglia circuits. Br. J. Pharmacol. 176 (8), 1156–1169. https://doi.org/10.1111/bph.14613.

Arbuthnott, G.W., Wickens, J., 2007. Space, time and dopamine. Trends Neurosci. 30 (2), 62–69. https://doi.org/10.1016/j.tins.2006.12.003.

Aristieta, A., Ruiz-Ortega, J.A., Miguelez, C., Morera-Herreras, T., Ugedo, L., 2016. Chronic L-DOPA administration increases the firing rate but does not reverse enhanced slow frequency oscillatory activity and synchronization in substantia nigra pars reticulata neurons from 6-hydroxydopamine-lesioned rats. Neurobiol. Dis. 89, 88–100. https://doi.org/10.1016/J.NBD.2016.02.003.

Aristieta, A., Ruiz-Ortega, J.A., Morera-Herreras, T., Miguelez, C., Ugedo, L., 2019. Acute L-DOPA administration reverses changes in firing pattern and low frequency oscillatory activity in the entopeduncular nucleus from long term L-DOPA treated 6-OHDA-lesioned rats. Exp. Neurol. 322, 113036. https://doi.org/10.1016/j.expneurol.2019.113036.

Atwood, B.K., Kupferschmidt, D.A., Lovinger, D.M., 2014. Opioids induce dissociable forms of long-term depression of excitatory inputs to the dorsal striatum. Nat. Neurosci. 17 (4), 540–548. https://doi.org/10.1038/nn.3652.

Benabid, A.L., Pollak, P., Gross, C., Hoffmann, D., Benazzouz, A., Gao, D.M., Laurent, A., Gentil, M., Perret, J., 1994. Acute and long-term effects of subthalamic nucleus stimulation of Parkinson's disease. Stereotact. Funct. Neurosurg. 62 (1–4), 76–84. https://doi.org/10.1159/000098600.

Bergman, H., Wichmann, T., Karmon, B., DeLong, M.R., 1994. The primate subthalamic nucleus. II. Neuronal activity in the MPTP model of parkinsonism. J. Neurophysiol. 72 (2), 507–520. https://doi.org/10.1152/jn.1994.72.2.507.

Beyeler, A., Kadiri, N., Navailles, S., Boujema, M.B., Gonon, F., Moine, C.L., Gross, C., De Deurwaerdère, P., 2010. Stimulation of serotonin2C receptors elicits abnormal oral movements by acting on pathways other than the sensorimotor one in the rat basal ganglia. Neuroscience 169 (1), 158–170. https://doi.org/10.1016/j.neuroscience.2010.04.061.

Braz, B.Y., Belforte, J.E., Murer, M.G., Galiñanes, G.L., 2017. Properties of the corticostriatal long term depression induced by medial prefrontal cortex high frequency stimulation in vivo. Neuropharmacology 121, 278–286. https://doi.org/10.1016/j.neuropharm.2017.05.001.

Carvalho, M.M., Campos, F.L., Coimbra, B., Pêgo, J.M., Rodrigues, C., Lima, R., Rodrigues, A.J., Sousa, N., Salgado, A.J., 2013. Behavioral characterization of the 6-hydroxidopamine model of Parkinson's disease and pharmacological rescuing of non-motor deficits. Mol. Neurodegener. 8 (1), 14. https://doi.org/10.1186/1750-1326-8-14.

Chan, C.S., Glajch, K.E., Gertler, T.S., Guzman, J.N., Mercer, J.N., Lewis, A.S., Goldberg, A.B., Tkatch, T., Shigemoto, R., Fleming, S.M., Chetkovich, D.M., Osten, P., Kita, H., Surmeier, D.J., 2011. HCN channelopathy in external globus pallidus neurons in models of Parkinson's disease. Nat. Neurosci. 14 (1), 85–92. https://doi.org/10.1038/nn.2692.

Ciliax, B.J., Heilman, C., Demchyshyn, L.L., Pristupa, Z.B., Ince, E., Hersch, S.M., Niznik, H.B., Levey, A.I., 1995. The dopamine transporter: immunochemical characterization and localization in brain. J. Neurosci. 15 (3), 1714–1723. https://doi.org/10.1523/JNEUROSCI.15-03-01714.1995.

Cragg, S.J., Rice, M.E., Greenfield, S.A., 1997. Heterogeneity of electrically evoked dopamine release and reuptake in substantia Nigra, ventral tegmental area, and striatum. J. Neurophysiol. 77 (2), 863–873. https://doi.org/10.1152/jn.1997.77.2.863.

Degos, B., Deniau, J.-M., Thierry, A.-M., Glowinski, J., Pezard, L., Maurice, N., 2005. Neuroleptic-induced catalepsy: electrophysiological mechanisms of functional recovery induced by high-frequency stimulation of the subthalamic nucleus. J. Neurosci. 25 (33), 7687–7696. https://doi.org/10.1523/JNEUROSCI.1056-05.2005.

Escande, M.V., Taravini, I.R.E., Zold, C.L., Belforte, J.E., Murer, M.G., 2016. Loss of homeostasis in the direct pathway in a mouse model of asymptomatic Parkinson's disease. J. Neurosci. 36 (21), 5686–5698. https://doi.org/10.1523/JNEUROSCI.0492-15.2016.

Farkas, S., Nagy, K., Jia, Z., Harkany, T., Palkovits, M., Donohou, S.R., Pike, V.W., Halldin, C., Máthé, D., Csiba, L., Gulyás, B., 2012. The decrease of dopamine D 2/D 3 receptor densities in the putamen and nucleus caudatus goes parallel with maintained levels of CB 1 cannabinoid receptors in Parkinson's disease: a preliminary autoradiographic study with the selective dopamine D 2/D 3 ant. Brain Res. Bull. 87 (6), 504–510. https://doi.org/10.1016/j.brainresbull.2012.02.012.

Ferré, S., Goldberg, S.R., Lluis, C., Franco, R., 2009. Looking for the role of cannabinoid receptor heteromers in striatal function. Neuropharmacology 56 (Suppl. 1), 226–234. https://doi.org/10.1016/j.neuropharm.2008.06.076.

Fieblinger, T., Graves, S.M., Sebel, L.E., Alcacer, C., Plotkin, J.L., Gertler, T.S., Chan, C.S., Heiman, M., Greengard, P., Cenci, M.A., Surmeier, D.J., 2014. Cell type-specific plasticity of striatal projection neurons in parkinsonism and L-DOPA-induced dyskinesia. Nat. Commun. 5 (1), 5316. https://doi.org/10.1038/ncomms6316.

Furlanetti, L.L., Coenen, V.A., Aranda, I.A., Döbrössy, M.D., 2015. Chronic deep brain stimulation of the medial forebrain bundle reverses depressive-like behavior in a hemiparkinsonian rodent model. Exp. Brain Res. 233 (11), 3073–3085. https://doi.org/10.1007/s00221-015-4375-9.

Gagnon, D., Petryszyn, S., Sanchez, M.G., Bories, C., Beaulieu, J.M., De Koninck, Y., Parent, A., Parent, M., 2017. Striatal neurons expressing D1 and D2 receptors are morphologically distinct and differently affected by dopamine denervation in mice. Sci. Rep. 7 (1), 41432. https://doi.org/10.1038/srep41432.

Galvan, A., Wichmann, T., 2008. Pathophysiology of parkinsonism. Clin. Neurophysiol. 119 (7), 1459–1474. https://doi.org/10.1016/j.clinph.2008.03.017.

García, C., Palomo-Garo, C., Gómez-Gálvez, Y., Fernández-Ruiz, J., 2016. Cannabinoid–dopamine interactions in the physiology and physiopathology of the basal ganglia. Br. J. Pharmacol. 173 (13), 2069–2079. https://doi.org/10.1111/bph.13215.

Giuffrida, A., Parsons, L.H., Kerr, T.M., Rodríguez de Fonseca, F., Navarro, M., Piomelli, D., 1999. Dopamine activation of endogenous cannabinoid signaling in dorsal striatum. Nat. Neurosci. 2 (4), 358–363. https://doi.org/10.1038/7268.

Grant, I., Gonzalez, R., Carey, C.L., Natarajan, L., Wolfson, T., 2003. Non-acute (residual) neurocognitive effects of cannabis use: a meta-analytic study. J. Int. Neuropsychol. Soc. 9 (5), 679–689. https://doi.org/10.1017/S1355617703950016.

Graves, S.M., Surmeier, D.J., 2019. Delayed spine pruning of direct pathway spiny projection neurons in a mouse model of Parkinson's disease. Front. Cell. Neurosci. 13, 32. https://doi.org/10.3389/fncel.2019.00032.

Haber, S.N., 2003. The primate basal ganglia: parallel and integrative networks. J. Chem. Neuroanat. 26 (4), 317–330. https://doi.org/10.1016/j.jchemneu.2003.10.003.

Hassani, O.K., Mouroux, M., Féger, J., 1996. Increased subthalamic neuronal activity after nigral dopaminergic lesion independent of disinhibition via the globus pallidus. Neuroscience 72 (1), 105–115. https://doi.org/10.1016/0306-4522(95)00535-8.

Heckman, P.R.A., Schweimer, J.V., Sharp, T., Prickaerts, J., Blokland, A., 2018. Phosphodiesterase 4 inhibition affects both the direct and indirect pathway: an electrophysiological study examining the tri-phasic response in the substantia nigra pars reticulata. Brain Struct. Funct. 223 (2), 739–748. https://doi.org/10.1007/s00429-017-1518-8.

Heilbronner, S.R., Rodriguez-Romaguera, J., Quirk, G.J., Groenewegen, H.J., Haber, S. N., 2016. Circuit-based corticostriatal homologies between rat and primate. Biol. Psychiatry 80 (7), 509–521. https://doi.org/10.1016/j.biopsych.2016.05.012.

Heng, L., Beverley, J.A., Steiner, H., Tseng, K.Y., 2011. Differential developmental trajectories for CB1 cannabinoid receptor expression in limbic/associative and sensorimotor cortical areas. Synapse 65 (4), 278–286. https://doi.org/10.1002/syn.20844.

Herkenham, M., Lynn, A.B., de Costa, B.R., Richfield, E.K., 1991. Neuronal localization of cannabinoid receptors in the basal ganglia of the rat. Brain Res. 547 (2), 267–274. https://doi.org/10.1016/0006-8993(91)90970-7.

Hernando, S., Requejo, C., Herran, E., Ruiz-Ortega, J.A., Morera-Herreras, T., Lafuente, J. V., Gainza, E., Pedraz, J.L., Igartua, M., Hernandez, R.M., 2019. Beneficial effects of n-3 polyunsaturated fatty acids administration in a partial lesion model of Parkinson's disease: the role of glia and NRf2 regulation. Neurobiol. Dis. 121, 252–262. https://doi.org/10.1016/j.nbd.2018.10.001.

Hohmann, A.G., Herkenham, M., 1999. Localization of central cannabinoid CB1 receptor messenger RNA in neuronal subpopulations of rat dorsal root ganglia: a double-label in situ hybridization study. Neuroscience 90 (3), 923–931. https://doi.org/10.1016/S0306-4522(98)00524-7.

Hohmann, Andrea G., Herkenham, M., 2000. Localization of cannabinoid CB1receptor mRNA in neuronal subpopulations of rat striatum: a double-label in situ hybridization study. Synapse 37 (1), 71–80. https://doi.org/10.1002/(SICI)1098-2396(200007)37:1<71::AID-SYN8>3.0.CO;2-K.

Hurley, M.J., Mash, D.C., Jenner, P., 2003. Expression of cannabinoid CB1 receptor mRNA in basal ganglia of normal and parkinsonian human brain. J. Neural Transm. (Vienna) 110 (11), 1279–1288. https://doi.org/10.1007/s00702-003-0033-7.

Irving, A.J., Coutts, A.A., Harvey, J., Rae, M.G., Mackie, K., Bewick, G.S., Pertwee, R.G., 2000. Functional expression of cell surface cannabinoid CB(1) receptors on presynaptic inhibitory terminals in cultured rat hippocampal neurons. Neuroscience 98 (2), 253–262. https://doi.org/10.1016/s0306-4522(00)00120-2.

Köfalvi, A., Rodrigues, R.J., Ledent, C., Mackie, K., Vizi, E.S., Cunha, R.A., Sperlágh, B., 2005. Involvement of cannabinoid receptors in the regulation of neurotransmitter release in the rodent striatum: a combined immunochemical and pharmacological analysis. J. Neurosci. 25 (11), 2874–2884. https://doi.org/10.1523/JNEUROSCI.4232-04.2005.

Kolomiets, B.P., Deniau, J.M., Glowinski, J., Thierry, A.M., 2003. Basal ganglia and processing of cortical information: functional interactions between trans-striatal and trans-subthalamic circuits in the substantia nigra pars reticulata. Neuroscience 117 (4), 931–938.

Lastres-Becker, I., Cebeira, M., De Ceballos, M.L., Zeng, B.Y., Jenner, P., Ramos, J.A., Fernández-Ruiz, J.J., 2001. Increased cannabinoid CB1 receptor binding and activation of GTP-binding proteins in the basal ganglia of patients with Parkinson's syndrome and of MPTP-treated marmosets. Eur. J. Neurosci. 14 (11), 1827–1832. https://doi.org/10.1046/j.0953-816X.2001.01812.x.

Lévesque, D., Martres, M.P., Diaz, J., Griffon, N., Lammers, C.H., Sokoloff, P., Schwartz, J.C., 1995. A paradoxical regulation of the dopamine D3 receptor expression suggests the involvement of an anterograde factor from dopamine neurons. Proc. Natl. Acad. Sci. 92 (5), 1719–1723. https://doi.org/10.1073/pnas.92.5.1719.

Linkert, M., Rueden, C.T., Allan, C., Burel, J.-M., Moore, W., Patterson, A., Loranger, B., Moore, J., Neves, C., Macdonald, D., Tarkowska, A., Sticco, C., Hill, E., Rossner, M., Eliceiri, K.W., Swedlow, J.R., 2010. Metadata matters: access to image data in the real world. J. Cell Biol. 189 (5), 777–782. https://doi.org/10.1083/jcb.201004104.

Magill, P.J., Bolam, J.P., Bevan, M.D., 2001. Dopamine regulates the impact of the cerebral cortex on the subthalamic nucleus–globus pallidus network. Neuroscience 106 (2), 313–330. https://doi.org/10.1016/S0306-4522(01)00281-0.

Mailleux, P., Vanderhaeghen, J.J., 1992. Localization of cannabinoid receptor in the human developing and adult basal ganglia. Higher levels in the striatonigral neurons. Neurosci. Lett. 148 (1–2), 173–176. https://doi.org/10.1016/0304-3940(92)90832-R.

Mallet, N., Ballion, B., Moine, C.L., Gonon, F., 2006. Cortical inputs and GABA interneurons imbalance projection neurons in the striatum of parkinsonian rats. J. Neurosci. 26 (14), 3875–3884. https://doi.org/10.1523/JNEUROSCI.4439-05.2006.

Marsicano, G., Lutz, B., 1999. Expression of the cannabinoid receptor CB1 in distinct neuronal subpopulations in the adult mouse forebrain. Eur. J. Neurosci. 11 (12), 4213–4225. https://doi.org/10.1046/j.1460-9568.1999.00847.x.

Martín, A.B., Fernandez-Espejo, E., Ferrer, B., Gorriti, M.A., Bilbao, A., Navarro, M., Rodriguez de Fonseca, F., Moratalla, R., 2008. Expression and function of CB 1 receptor in the rat striatum: localization and effects on D 1 and D 2 dopamine receptor-mediated motor behaviors. Neuropsychopharmacology 33 (7), 1667–1679. https://doi.org/10.1038/sj.npp.1301558.

Matsuda, L.A., Bonner, T.I., Lolait, S.J., 1993. Localization of cannabinoid receptor mRNA in rat brain. J. Comp. Neurol. 327 (4), 535–550. https://doi.org/10.1002/cne.903270406.

Maurice, N., Deniau, J.-M., Glowinski, J., Thierry, A.-M., 1999. Relationships between the prefrontal cortex and the basal ganglia in the rat: physiology of the Cortico-Nigral circuits. J. Neurosci. 19 (11), 4674–4681. https://doi.org/10.1523/JNEUROSCI.19-11-04674.1999.

Maurice, N., Deltheil, T., Melon, C., Degos, B., Mourre, C., Amalric, M., Goff, L.K.L., 2015. Bee venom alleviates motor deficits and modulates the transfer of cortical information through the basal ganglia in rat models of Parkinson's disease. PLoS One 10 (11). https://doi.org/10.1371/journal.pone.0142838.

McGeorge, A.J., Faull, R.L., 1989. The organization of the projection from the cerebral cortex to the striatum in the rat. Neuroscience 29 (3), 503–537.

Meissner, W., Ravenscroft, P., Reese, R., Harnack, D., Morgenstern, R., Kupsch, A., Klitgaard, H., Bioulac, B., Gross, C.E., Bezard, E., Boraud, T., 2006. Increased slow oscillatory activity in substantia nigra pars reticulata triggers abnormal involuntary movements in the 6-OHDA-lesioned rat in the presence of excessive extracelullar striatal dopamine. Neurobiol. Dis. 22 (3), 586–598. https://doi.org/10.1016/j.nbd.2006.01.009.

Middleton, F.A., Strick, P.L., 2000. Basal ganglia output and cognition: evidence from anatomical, behavioral, and clinical studies. Brain Cogn. 42 (2), 183–200. https://doi.org/10.1006/brcg.1999.1099.

Miguelez, C., Morin, S., Martinez, A., Goillandeau, M., Bezard, E., Bioulac, B., Baufreton, J., 2012. Altered pallido-pallidal synaptic transmission leads to aberrant firing of globus pallidus neurons in a rat model of Parkinson's disease. J. Physiol. 590 (22), 5861–5875. https://doi.org/10.1113/jphysiol.2012.241331.

Morera-Herreras, T., Ruiz-Ortega, J.A., Linazasoro, G., Ugedo, L., 2011. Nigrostriatal denervation changes the effect of cannabinoids on subthalamic neuronal activity in rats. Psychopharmacology 214 (2), 379–389. https://doi.org/10.1007/s00213-010-2043-0.

Morera-Herreras, T., Miguelez, C., Aristieta, A., Ruiz-Ortega, J.Á., Ugedo, L., 2012. Endocannabinoid modulation of dopaminergic motor circuits. Front. Pharmacol. 3, 110. https://doi.org/10.3389/fphar.2012.00110.

Murer, M.G., Riquelme, L.A., Tseng, K.Y., Pazo, J.H., 1997. Substantia nigra pars reticulata single unit activity in normal and 60HDA-lesioned rats: effects of intrastriatal apomorphine and subthalamic lesions. Synapse 27 (4), 278–293. https://doi.org/10.1002/(SICI)1098-2396(199712)27:4<278::AID-SYN2>3.0.CO;2-9.

Oorschot, D.E., Tunstall, M.J., Wickens, J.R., 2002. Local connectivity between striatal spiny projection neurons: a re-evaluation. In: Nicholson, L.F.B., Faull, R.L.M. (Eds.),

The Basal Ganglia VII. Springer US. https://doi.org/10.1007/978-1-4615-0715-4_42 (pp. 421–434).
Parent, A., Hazrati, L.N., 1995. Functional anatomy of the basal ganglia. I. The cortico-basal ganglia-thalamo-cortical loop. Brain Res. Rev. 20 (1), 91–127. https://doi.org/10.1016/0165-0173(94)00007-C.
Patel, S., Rademacher, D.J., Hillard, C.J., 2003. Differential regulation of the endocannabinoids anandamide and 2-arachidonylglycerol within the limbic forebrain by dopamine receptor activity. J. Pharmacol. Exp. Ther. 306 (3), 880–888. https://doi.org/10.1124/jpet.103.054270.
Paxinos, G., Watson, C., 2006. The Rat Brain in Stereotaxic Coordinates, Vol. 2. Academic Press. https://books.google.com/books?id=0prYfdDbh58C&pgis=1.
Prashad, S., Filbey, F.M., 2017. Cognitive motor deficits in cannabis users. Curr. Opin. Behav. Sci. 13, 1–7. https://doi.org/10.1016/j.cobeha.2016.07.001.
Rajakumar, N., Rushlow, W., Naus, C.C.G., Elisevich, K., Flumerfelt, B.A., 1994. Neurochemical compartmentalization of the globus pallidus in the rat: an immunocytochemical study of calcium-binding proteins. J. Comp. Neurol. 346 (3), 337–348. https://doi.org/10.1002/cne.903460303.
Rice, M.E., Richards, C.D., Nedergaard, S., Hounsgaard, J., Nicholson, C., Greenfield, S. A., 1994. Direct monitoring of dopamine and 5-HT release in substantia nigra and ventral tegmental area in vitro. Exp. Brain Res. 100 (3), 395–406. https://doi.org/10.1007/BF02738400.
Rice, M.E., Cragg, S.J., Greenfield, S.A., 1997. Characteristics of electrically evoked somatodendritic dopamine release in substantia nigra and ventral tegmental area in vitro. J. Neurophysiol. 77 (2), 853–862. https://doi.org/10.1152/jn.1997.77.2.853.
Rojo-Bustamante, E., Abellanas, M.A., Clavero, P., Thiolat, M.L., Li, Q., Luquin, M.R., Bezard, E., Aymerich, M.S., 2018. The expression of cannabinoid type 1 receptor and 2-arachidonoyl glycerol synthesizing/degrading enzymes is altered in basal ganglia during the active phase of levodopa-induced dyskinesia. Neurobiol. Dis. 118, 64–75. https://doi.org/10.1016/j.nbd.2018.06.019.
Romero, J., Berrendero, F., Pérez-Rosado, A., Manzanares, J., Rojo, A., Fernández-Ruiz, J.J., de Yebenes, J.G., Ramos, J.A., 2000. Unilateral 6-hydroxydopamine lesions of nigrostriatal dopaminergic neurons increased CB1 receptor mRNA levels in the caudate-putamen. Life Sci. 66 (6), 485–494. https://doi.org/10.1016/S0024-3205(99)00618-9.
Romero, Julián, Lastres-Becker, I., De Miguel, R., Berrendero, F., Ramos, J.A., Fernández-Ruiz, J., 2002. The endogenous cannabinoid system and the basal ganglia: biochemical, pharmacological, and therapeutic aspects. Pharmacol. Ther. 95 (2), 137–152. https://doi.org/10.1016/S0163-7258(02)00253-X.
Sano, H., Nambu, A., 2019. The effects of zonisamide on L-DOPA–induced dyskinesia in Parkinson's disease model mice. Neurochem. Int. 124, 171–180. https://doi.org/10.1016/j.neuint.2019.01.011.
Schindelin, J., Arganda-Carreras, I., Frise, E., Kaynig, V., Longair, M., Pietzsch, T., Preibisch, S., Rueden, C., Saalfeld, S., Schmid, B., Tinevez, J.-Y., White, D.J., Hartenstein, V., Eliceiri, K., Tomancak, P., Cardona, A., 2012. Fiji: an open-source platform for biological-image analysis. Nat. Methods 9 (7), 676–682. https://doi.org/10.1038/nmeth.2019.
Schreiner, A.M., Dunn, M.E., 2012. Residual effects of cannabis use on neurocognitive performance after prolonged abstinence: a meta-analysis. Exp. Clin. Psychopharmacol. 20 (5), 420–429. https://doi.org/10.1037/a0029117.
Sharman, M., Valabregue, R., Perlbarg, V., Marrakchi-Kacem, L., Vidailhet, M., Benali, H., Brice, A., Lehéricy, S., 2013. Parkinson's disease patients show reduced cortical-subcortical sensorimotor connectivity. Mov. Disord. 28 (4), 447–454. https://doi.org/10.1002/mds.25255.
Singh, A., Mewes, K., Gross, R.E., DeLong, M.R., Obeso, J.A., Papa, S.M., 2016. Human striatal recordings reveal abnormal discharge of projection neurons in Parkinson's disease. Proc. Natl. Acad. Sci. U. S. A. 113 (34), 9629–9634. https://doi.org/10.1073/pnas.1606792113.
Steigerwald, F., Pötter, M., Herzog, J., Pinsker, M., Kopper, F., Mehdorn, H., Deuschl, G., Volkmann, J., 2008. Neuronal activity of the human subthalamic nucleus in the parkinsonian and nonparkinsonian state. J. Neurophysiol. 100 (5), 2515–2524. https://doi.org/10.1152/jn.90574.2008.
Suarez, L.M., Solis, O., Aguado, C., Lujan, R., Moratalla, R., 2016. L-DOPA oppositely regulates synaptic strength and spine morphology in D1 and D2 striatal projection neurons in dyskinesia. Cereb. Cortex 26 (11), 4253–4264. https://doi.org/10.1093/cercor/bhw263.
Tremblay, L., Worbe, Y., Thobois, S., Sgambato-Faure, V., Féger, J., 2015. Selective dysfunction of basal ganglia subterritories: from movement to behavioral disorders. Mov. Disord. 30 (9), 1155–1170. https://doi.org/10.1002/mds.26199.
Tseng, K.Y., Riquelme, L.A., Belforte, J.E., Pazo, J.H., Murer, M.G., 2000. Substantia nigra pars reticulata units in 6-hydroxydopamine-lesioned rats: responses to striatal D2 dopamine receptor stimulation and subthalamic lesions. Eur. J. Neurosci. 12 (1), 247–256. https://doi.org/10.1046/j.1460-9568.2000.00910.x.
Tsou, K., Brown, S., Sañudo-Peña, M.C., Mackie, K., Walker, J.M., 1998. Immunohistochemical distribution of cannabinoid CB1 receptors in the rat central nervous system. Neuroscience 83 (2), 393–411. https://doi.org/10.1016/S0306-4522(97)00436-3.
Van Waes, V., Beverley, J.A., Siman, H., Tseng, K.Y., Steiner, H., 2012. CB1 cannabinoid receptor expression in the striatum: association with Corticostriatal circuits and developmental regulation. Front. Pharmacol. 3, 21. https://doi.org/10.3389/fphar.2012.00021.
Vegas-Suárez, S., Pisanò, C.A., Requejo, C., Bengoetxea, H., Lafuente, J.V., Morari, M., Miguelez, C., Ugedo, L., 2020. 6-Hydroxydopamine lesion and levodopa treatment modify the effect of buspirone in the substantia nigra pars reticulata. Br. J. Pharmacol. 177 (17), 3957–3974. https://doi.org/10.1111/bph.15145.
Voorn, P., Vanderschuren, L.J.M.J., Groenewegen, H.J., Robbins, T.W., Pennartz, C.M.A., 2004. Putting a spin on the dorsal-ventral divide of the striatum. Trends Neurosci. 27 (8), 468–474. https://doi.org/10.1016/j.tins.2004.06.006.
Wall, N.R., De La Parra, M., Callaway, E.M., Kreitzer, A.C., 2013. Differential innervation of direct- and indirect-pathway striatal projection neurons. Neuron 79 (2), 347–360. https://doi.org/10.1016/j.neuron.2013.05.014.
Walsh, S., Mnich, K., Mackie, K., Gorman, A.M., Finn, D.P., Dowd, E., 2010. Loss of cannabinoid CB1receptor expression in the 6-hydroxydopamine-induced nigrostriatal terminal lesion model of Parkinson's disease in the rat. Brain Res. Bull. 81 (6), 543–548. https://doi.org/10.1016/j.brainresbull.2010.01.009.
Wang, Y., Zhang, Q.J., Liu, J., Ali, U., Gui, Z.H., Hui, Y.P., Chen, L., Wang, T., 2010. Changes in firing rate and pattern of GABAergic neurons in subregions of the substantia nigra pars reticulata in rat models of Parkinson's disease. Brain Res. 1324, 54–63. https://doi.org/10.1016/j.brainres.2010.02.008.
Weiss-Wunder, L.T., Chesselet, M.-F., 1990. Heterogeneous distribution of cytochrome oxidase activity in the rat substantia nigra: correlation with tyrosine hydroxylase and dynorphin immunoreactivities. Brain Res. 529 (1), 269–276. https://doi.org/10.1016/0006-8993(90)90837-2.
Winter, C., von Rumohr, A., Mundt, A., Petrus, D., Klein, J., Lee, T., Morgenstern, R., Kupsch, A., Juckel, G., 2007. Lesions of dopaminergic neurons in the substantia nigra pars compacta and in the ventral tegmental area enhance depressive-like behavior in rats. Behav. Brain Res. 184 (2), 133–141. https://doi.org/10.1016/j.bbr.2007.07.002.
Yung, K.K.L., Bolam, J.P., Smith, A.D., Hersch, S.M., Ciliax, B.J., Levey, A.I., 1995. Immunocytochemical localization of D1 and D2 dopamine receptors in the basal ganglia of the rat: light and electron microscopy. Neuroscience 65 (3), 709–730. https://doi.org/10.1016/0306-4522(94)00536-E.
Zeng, B.Y., Dass, B., Owen, A., Rose, S., Cannizzaro, C., Tel, B.C., Jenner, P., 1999. Chronic L-DOPA treatment increases striatal cannabinoid CB1 receptor mRNA expression in 6-hydroxydopamine-lesioned rats. Neurosci. Lett. 276 (2), 71–74. https://doi.org/10.1016/S0304-3940(99)00762-4.
Zhang, X., Egeland, M., Svenningsson, P., 2011. Antidepressant-like properties of sarizotan in experimental parkinsonism. Psychopharmacology 218 (4), 621–634. https://doi.org/10.1007/s00213-011-2356-7.
Zimmer, A., Steiner, H., Bonner, T.I., Zimmer, A.M., Kitai, S.T., 1999. Altered gene expression in striatal projection neurons in CB1 cannabinoid receptor knockout mice. Proc. Natl. Acad. Sci. U. S. A. 96 (10), 5786–5790. https://doi.org/10.1073/pnas.96.10.5786.